The Geological Society of America
Field Guide 39
2015

A road guide to the Harpeth River and Stones River fault zones on the northwest flank of the Nashville dome, central Tennessee

Mark Abolins*
Department of Geosciences, Middle Tennessee State University, Murfreesboro, Tennessee 37132, USA

Shaunna Young
Geology Department, Radford University, Radford, Virginia 24141, USA

Joe Camacho[†]
Environmental Science and Management, Humboldt State University, Arcata, California 95521, USA

Mark Trexler[#]
Alex Ward**
Matt Cooley[††]
Albert Ogden
Department of Geosciences, Middle Tennessee State University, Murfreesboro, Tennessee 37132, USA

ABSTRACT

The authors use mesoscale structures and existing 1:24,000 scale geologic maps to infer the locations of four macroscale NNW-striking blind normal faults on the northwest flank of the Nashville dome ~30 km south of downtown Nashville. The Harpeth River fault zone has an across-strike width of ~6 km, and, from west to east, includes the Peytonsville, Arno, McClory Creek, and McDaniel fault zones. All of the fault zones are east-side-down except for the west-side-down Peytonsville fault zone. Mesoscale structures are exposed within each fault zone and are observed at three stops along Tennessee State Route (S.R.)-840 and at an additional stop 1.8 km south of the highway. These structures include minor normal faults (maximum dip separation 3.8 m), non-vertical joints, and mesoscale folds. No faults are depicted on existing geologic maps of the zone, but these maps reveal macroscale folding of the contact between the Ordovician Carters Formation and the overlying Hermitage Formation. The authors use the orientation and amplitude of these folds to constrain the orientation and length of the inferred blind fault zones and the amount of structural relief

*Mark.Abolins@mtsu.edu
[†]Current address: IslandWood, 4450 Blakely Avenue, NE, Bainbridge Island, Washington 98110, USA.
[#]Current address: Environmental Sciences Corporation Lab Sciences, 12065 Lebanon Road, Mt. Juliet, Tennessee 37122, USA.
**Current address: Department of Earth Sciences, University of Memphis, Memphis, Tennessee 38152, USA.
[††]Current address: Center for Earthquake Research and Information, University of Memphis, Memphis, Tennessee 38152, USA.

Abolins, M., Young, S., Camacho, J., Trexler, M., Ward, A., Cooley, M., and Ogden, A., 2015, A road guide to the Harpeth River and Stones River fault zones on the northwest flank of the Nashville dome, central Tennessee, *in* Holmes, A.E., ed., Diverse Excursions in the Southeast: Paleozoic to Present: Geological Society of America Field Guide 39, p. 1–20, doi:10.1130/2015.0039(01). For permission to copy, contact editing@geosociety.org.

across the zones. The longest fault zones are the Arno (13.2 km long) and McDaniel (11.6 km) fault zones, and the amount of structural relief across these zones peaks at 27 m and 24 m, respectively.

The authors also use existing geologic maps to hypothesize that a second east-side-down blind normal fault zone (Stones River fault zone) is located ~27 km northeast of the Harpeth River fault zone. The authors interpret non-vertical joints at one stop as fault-related, and they interpret joints at a second stop as related to a hanging wall syncline. Both of these stops are within 4 km of S.R.-840.

INTRODUCTION

The Nashville dome is the southern extension of the Cincinnati Arch, a regional uplift largely related to Paleozoic flexure of the lithosphere during orogenic loading of the Laurentian margin (Beaumont et al., 1988; Holland and Patzkowsky, 1997). Joints and gentle folds are widespread in the dome, and minor faults are exposed at a few locations (e.g., Galloway, 1919; Wilson and Stearns, 1963; Wilson, 1964, 1991; Bordine, 1977). Many of these structures are plausibly related to the Paleozoic to Cenozoic uplift of the dome or the Paleozoic uplift of the Appalachian Mountains. For example, folds having hinges parallel to the ~045–050° trend of the dome and the southern Appalachian Mountains plausibly formed in connection with Paleozoic contraction. In addition, it might be reasonable to speculate that folds having hinges perpendicular to the trend of the dome are also somehow dome-related, because orthogonal folds are common in gneiss domes (e.g., Yin, 2004). Likewise, joint sets striking parallel to and perpendicular to the trend of the Appalachians plausibly formed through the processes of pressure release and syntectonic hydrofracture, respectively. However, the bearing of some fold hinges (Moore et al., 1969) and the strike of some joints (e.g., Matthews, 1971) and minor faults is 340–010°, and the origin of these structures is not obvious, because they are oriented at an oblique angle with respect to the Nashville dome and the Appalachian Mountains.

One possible explanation for the origin of the oblique folds and joints is that they formed in response to movement on blind basement faults. Although no basement structures appear within the Nashville dome on the *Precambrian Basement Structure Map of the Continental United States* (Sims et al., 2008), Stearns and Reesman (1986) used drill hole and magnetic anomaly data to infer depth to magnetic basement, and they hypothesized that Precambrian rifting was responsible for variations in depth. Then, Johnson et al. (1994) used potential-field data to map a hypothetical graben immediately west of the dome. Marshak and Paulsen (1996) hypothesized that many Paleozoic and younger midcontinent U.S. fault and fold zones developed through reactivation of Precambrian rift faults, and Marshak et al. (2000) specifically hypothesized that many midcontinent Paleozoic uplifts formed through inversion of Precambrian rifts, although the Nashville dome is not depicted as a rift on tectonic maps in these two papers. Most recently, Liang and Langston (2009) used a crustal velocity model to hypothesize that the dome coincides with a Precambrian rift. If there are Precambrian normal faults in the basement below the Nashville dome, they may have reactivated during the Phanerozoic to accommodate minor extension during uplift of the dome. In general, joints and minor faults and a monocline or an asymmetric anticline form up-dip from a blind normal fault, and a syncline develops on the hanging wall (Fig. 1). Conjugate fractures form in the footwall in physical analog experiments (e.g., Withjack et al., 1990) and have been observed in the field (e.g., Jackson et al., 2006).

This study examined two areas where fold hinges and fractures are oblique to the trend of the dome. These areas are located south and southeast of Nashville, Tennessee (Fig. 2).

Harpeth River Syncline

One area is located a little more than 30 km south-southeast of Nashville and is broadly coincident with part of the Harpeth River watershed. Within this area, strata are at a lower elevation than the same strata where they crop out to the southwest and northeast along the trend of the dome (Wilson and Stearns,

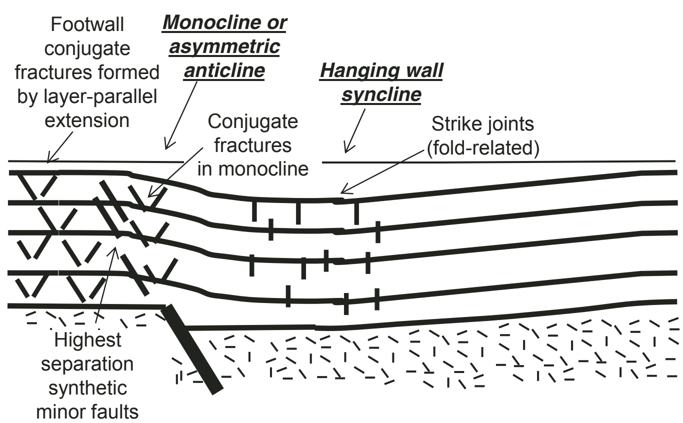

Figure 1. Conceptual model of the relationship between a macroscale monocline (or asymmetric anticline) and syncline, minor faults, and joints observed at the surface, on the one hand, and a blind basement normal fault, on the other hand. The model is mostly based on physical analog experiments (e.g., Withjack et al., 1990) and field studies within the Red Sea rift (Sharp et al., 2000; Jackson et al., 2006), Gulf of California (Willsey et al., 2002), Basin and Range Province (Berg and Skar, 2005), and Colorado Plateau (Resor, 2008). No particular scale is implied.

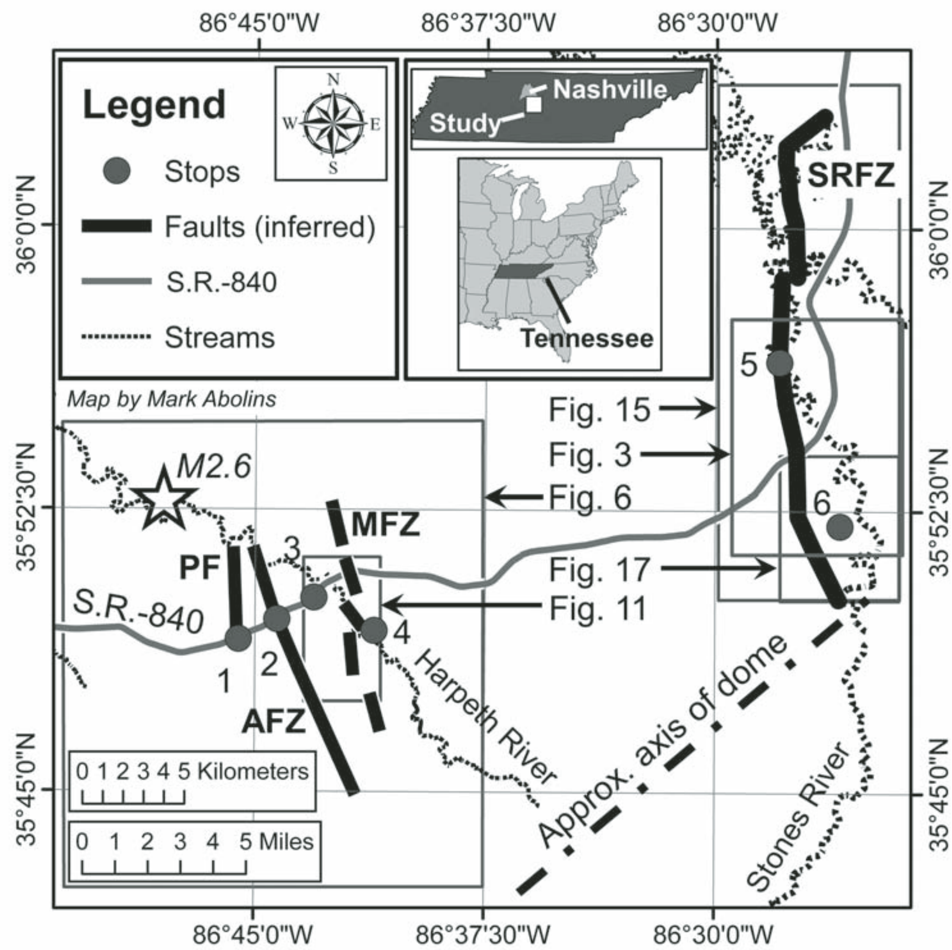

Figure 2. Location of stops (numbered 1–6) and index of figures in relation to Tennessee S.R.-840, the Harpeth and Stones Rivers, hypothetical basement faults, the approximate axis of the Nashville dome (Wilson and Stearns, 1963; Stearns and Reesman, 1986), and the epicenter of the 8 July 2001 M2.6 earthquake. All faults are high-angle normal faults, and all are east-side-down except for the Peytonsville fault, which is west-side-down. Inset shows location in relation to Nashville, Tennessee, and the rest of the eastern United States. PF—Peytonsville fault; AFZ—Arno fault zone; MFZ—McDaniel fault zone; SRFZ—Stones River fault zone. The McClory Creek fault zone (MCFZ) is at Stop 3 and is too small to depict at this scale. Together, the PF, AFZ, MCFZ, and MFZ comprise the Harpeth River fault zone.

1963; Wilson et al., 1963; Miller and McCary, 1963), indicating a syncline (Harpeth River syncline) oblique to the trend of the dome. Within this syncline, construction of Tennessee State Route (S.R.) 840 around the year 2000 revealed minor normal faults, non-vertical joints, and mesoscale folds at three locations.

Stones River Syncline

The second area is broadly coincident with part of the Stones River watershed a little more than 30 km southeast of Nashville (Fig. 2). In the second area, a 17-km-long north-south belt of the relatively young Ordovician Lebanon limestone is surrounded by older strata of the Ordovician Ridley and Murfreesboro limestones, defining the Stones River syncline. Along the western edge of the syncline, Galloway (1919) mapped a minor normal fault at a location now submerged beneath Percy Priest Reservoir, and Wilson (1964) mapped a minor normal fault near the same location.

Within the Stones River syncline, numerous dye traces (Fig. 3) suggest that groundwater flows through fractures striking at an angle oblique to the trend of the dome and approximately parallel to the hinge of the syncline. These dye traces define a 6-km-long belt in which groundwater flows north along bearings of 341° to 020°. In contrast, groundwater in surrounding areas mostly moves northwest along bearings of 282–341° and northeast along bearings of 038–072°, and a pair of traces indicate flow to the southeast along bearings of 139° and 143°. The northwest and southeast flow is broadly consistent with flow through a widespread joint set striking approximately perpendicular to the trend of the Nashville dome and the Appalachian Mountains, and the northeast flow is broadly consistent with flow through a set striking parallel to the regional structures.

Field Trip Stops

Mesoscale faults are exposed at the Harpeth River syncline stops (1–4), but not at the Stones River syncline stops (5 and 6). At the first four stops (Fig. 2), participants will examine minor normal faults, mesoscale folds, and joints along a WSW-ENE transect oriented approximately perpendicular to the strike of the inferred faults. At these stops, road guide readers will evaluate the hypothesis that the minor fractures and mesoscale folds formed through movement on larger blind normal faults. From WSW to ENE, the four exposed fault zones are the Peytonsville

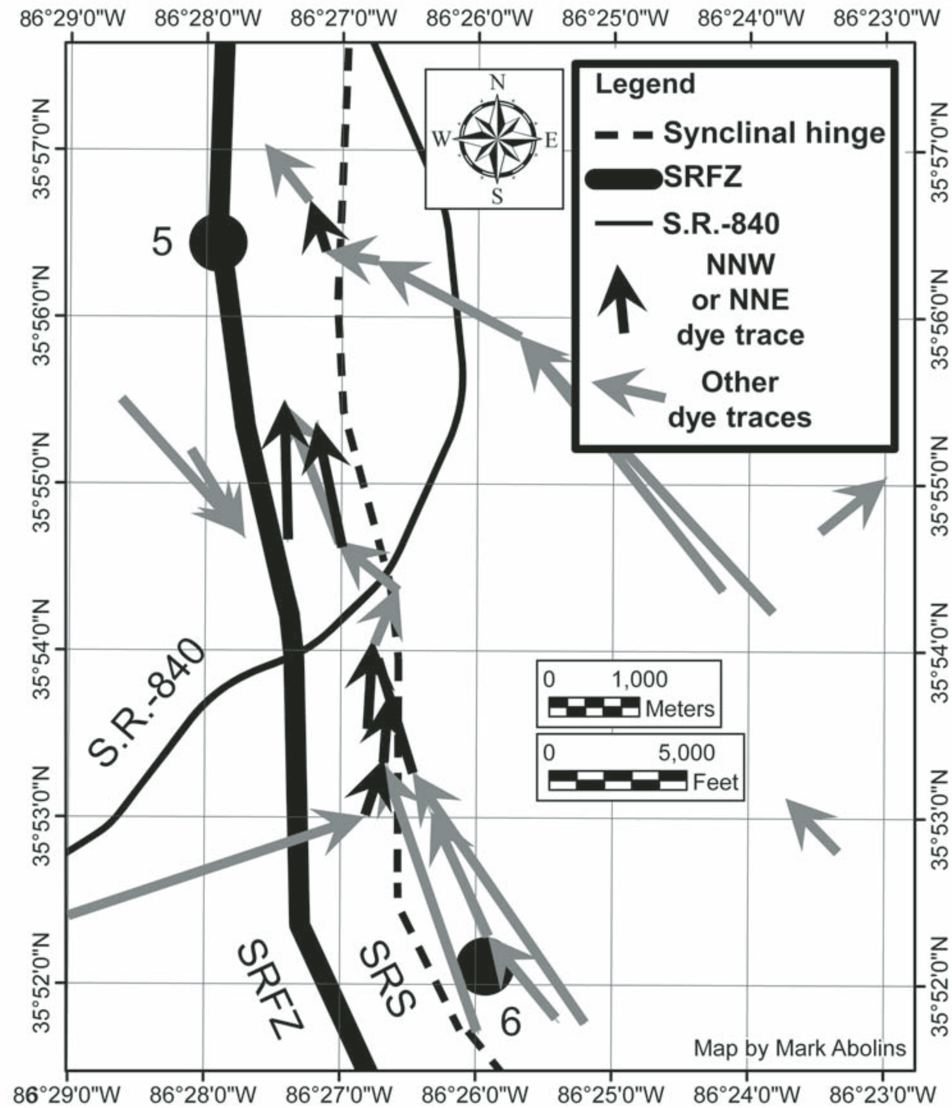

Figure 3. Groundwater dye traces in relation to Stops 5 and 6, the approximate hinge of the Stones River syncline (SRS) (Wilson and Hughes, 1963; Wilson, 1964, 1965; Moore et al., 1969), and the hypothetical Stones River fault zone (SRFZ) (this paper). See Figure 2 for the location of this figure in relation to the rest of the study area. Dye traces are described in Crawford (1988), Ogden and Scott (1998), Ogden et al. (1998, 1999, 2001, 2002), and Ogden and Powell (1999).

(Stop 1), Arno (Stop 2), McClory Creek (Stop 3), and McDaniel (Stop 4), and the entire zone (Harpeth River fault zone) is a little less than 6 km wide along the field trip route. Geologic mapping (Wilson et al., 1963; Miller and McCary, 1963) shows that the Arno and McDaniel fault zones are associated with the largest amount of structural relief (peaking at 27 m and 24 m, respectively), but the largest vertical offsets are visible in the Arno and Peytonsville fault zones (3.8 m and 1.1 m, respectively). All of these fault zones are predominantly east-side-down except for the Peytonsville fault zone, which is west-side-down. Geologic mapping shows that the Arno fault zone (Stop 2) is coincident with the western edge of the Harpeth River syncline, and that the stops are located along the northwestern periphery of the Nashville dome.

The last two stops are in the Stones River syncline, and no minor faults are exposed at these stops. However, in light of structures observed at Stops 1–4, the geology of the Stones River syncline (Galloway, 1919; Wilson and Hughes, 1963; Wilson, 1964, 1965; Moore et al., 1969), and groundwater dye trace data (Fig. 3), the authors hypothesize that a fault zone (Stones River fault zone) underlies the western edge of the Stones River syncline and that the syncline is a hanging wall syncline. Joints striking 348° and dipping 78°E at Stop 5 are the principal mesoscale structures interpreted as fault-related. At Stop 6, NNW- and ENE-striking joints are exposed in a N-plunging fold hinge ~600 m NE of the Stones River syncline hinge. The authors interpret the fold at Stop 6 as parasitic on the Stones River syncline, and the authors interpret the joints as fold-related.

Dissolution widened these joints into fissures, creating natural trenches, and a cedar forest grows atop the area. The fissures and trees were used as protection by Union soldiers on the morning of 31 December 1862 during the American Civil War Battle of Stones River (e.g., McDonough, 1989; Daniel, 2012). Union soldiers held out in this defensive position throughout much of the morning, although Confederate soldiers took the position by noon. Casualties were high on both sides and some Union units lost one third of their men, providing a spectacular example of the connection between karst and Civil War casualties noted at other battlefields by Robert Whisonant and Judy Ehlen (Wayman, 2008).

GEOLOGIC SETTING OF THE NASHVILLE DOME

In the Nashville dome area, ca. 1.38 Ga granite basement (Fisher et al., 2010) is overlain by ~1.7 km of Cambrian to Mississippian strata (Ryder, 1987). The faults observed at Stops 1–4 cut the Ordovician Carters and Hermitage Formations, and the joints observed at Stops 5 and 6 cut the Ordovician Ridley limestone. (See Fig. 4 for a stratigraphic column.) The basement is likely ~1.4 km below these stops, although depth may vary because of erosional relief on the top of the basement (e.g., Mallory, 1974).

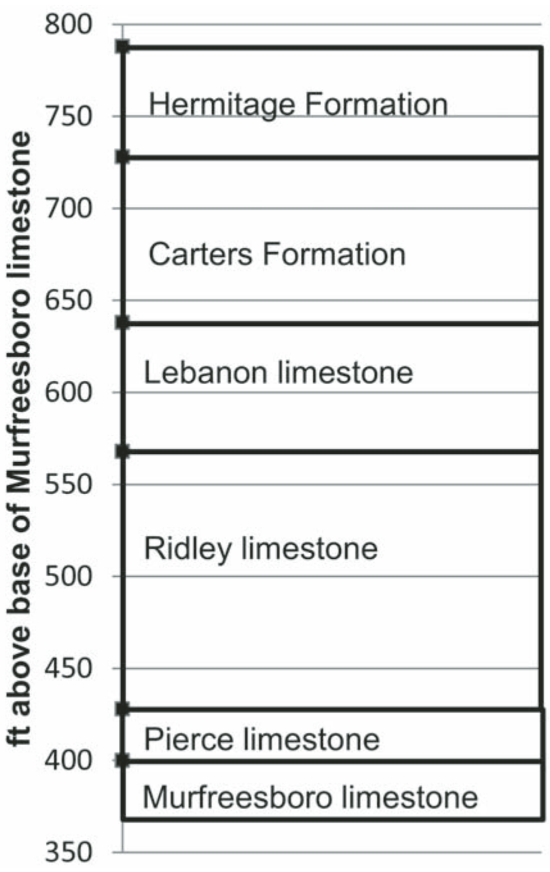

Figure 4. Generalized stratigraphic column showing approximate thicknesses of Ordovician formations within the study area. Note that only the upper few feet of the Murfreesboro limestone are exposed, although the formation is ~400 ft thick. (Sources: Miller and McCary [1963], Wilson et al. [1963], and Farmer and Hollyday [1999].)

The Nashville dome formed during several episodes of uplift beginning in the Middle Ordovician (roughly synchronous with the Taconic orogeny) and continuing through the Cenozoic (Wilson and Stearns, 1963). The largest amount of uplift happened during the late Mississippian and Pennsylvanian and was roughly synchronous with the Alleghanian orogeny. Most of the uplift was likely caused by flexure of the lithosphere due to orogenic loading of the Laurentian margin (Beaumont et al., 1988; Holland and Patzkowsky, 1997), although Reesman and Stearns (1989) attribute some of the uplift to isostatic adjustments related to erosional unloading of the dome itself.

The mesoscale faults and folds described at each stop are all post-formational, and, consequently, postdate the Ordovician Taconic orogeny. However, the T3 (Deicke) K-bentonite, the unconformable Carters-Hermitage contact, and soft-sediment deformation in the Hermitage Formation at Stops 2 and 3 are broadly synchronous with the orogeny. Bentonites in central Tennessee, Kentucky, and Alabama yielded Ar-Ar biotite ages of 454.1 ± 3.1 Ma and 455.1 ± 4.9 Ma (Kunk and Sutter, 1984), making them synchronous with the orogeny. Although Min et al. (2001) criticized these Ar-Ar ages, more recent U-Pb dating of the Deicke bentonite in Kentucky (Renne et al., 2010) indicates an age of 454.59 ± 0.56, which is still synchronous with the Taconic orogeny. Holland and Patzkowsky (1997) believed uplift due to lithospheric flexure caused the unconformity at the base of the Hermitage Formation, and they thought soft-sediment deformation in the Hermitage Formation was caused by seismic activity.

The Harpeth River and Stones River fault zones are almost completely aseismic today, but an M2.6 earthquake happened ~8 km northwest of Stop 1 along a bearing of 332° on 8 July 2001 UTC (7 July local date). Note, however, that the Tennessee Valley Authority (TVA) network estimated the epicentral location and that central Tennessee does not have a permanent seismograph network. Consequently, the location is not precise.

During 2013–2014, the magnetic declination at Stops 1–4 was 3.4–3.5° according to the National Geophysical Data Center magnetic field calculators Web page (www.ngdc.noaa.gov/geomag-web/#declination), and a magnetic declination of 3° was used for all measurements described under these stops. For Stops 5 and 6, a magnetic declination of 4° was used because the magnetic declination was ~3.7°.

MEASURING THE STRIKE AND DIP OF GENTLY DIPPING BEDDING PLANES

The authors have used a Macklanburg-Duncan SmartTool 24-inch digital level and Brunton pocket transit to measure the strike and dip of bedding at numerous locations in central Tennessee. To make a measurement, they placed a nonmagnetic metal sheet or plastic cutting board on a bed top, and then they placed the level on the sheet or board. To find the strike, they rotated the level until the dip read 0.0°, and then they used a right triangle to find the dip direction. Figure 5A shows the level and right triangle (left) and the level reading 0.0° (right). After positioning

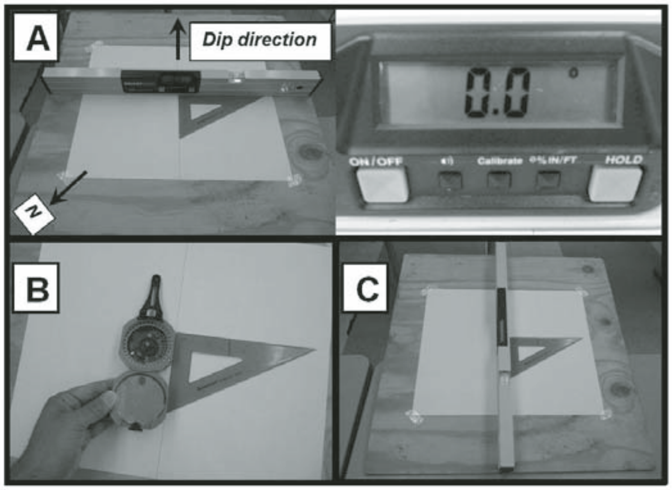

Figure 5. Measuring a bedding plane attitude with a digital level and Brunton pocket transit. See text for more information. (A) Finding the strike, (B) measuring the dip azimuth, and (C) measuring the dip.

the level and right triangle as shown in Figure 5A, they used a Brunton compass to measure the dip azimuth (Fig. 5B). After measuring the dip azimuth, they placed the level in alignment with the dip azimuth, and they read the dip off of the digital level (Fig. 5C). Wherever possible, they made multiple measurements on the same bed top and averaged the measurements.

Abolins (2014) showed that the measurement technique described in the above paragraph produces reproducible results revealing previously unmapped folds.

ROAD GUIDE

Stop 1. Peytonsville Fault, TN S.R.-840 East of Peytonsville Exit

(0.8 road mi east of the Peytonsville exit on S.R.-840; 521679 m E, 3963749 m N, UTM Zone 16)

Park at the "Arno Road 1 mile" sign on the broad shoulder for the eastbound lanes.

The Peytonsville minor normal fault has the second largest dip separation (~1.1 m down-to-the-west) of any normal fault in the Harpeth River fault zone. The fault is ~1.7 km WSW of the western edge of the Harpeth River syncline. The fault is typical of faults in the zone: it is steeply dipping (64° W), and strikes slightly NNW (351°). Geologic mapping (Fig. 6) suggests that the fault exposed in outcrop is above the southern end of a roughly 4.7 km, NNW-striking west-side-down blind normal fault.

A second minor normal fault having ~24 cm of dip separation is exposed in the hanging wall of the Peytonsville fault on the north side of S.R.-840 but not on the south side.

A mesoscale syncline having limbs dipping less than 9° is exposed ~60 m southwest of the fault. Bedding measured near the fault in the footwall on the north side of S.R.-840 strikes approximately parallel to the fault and has a relatively steep dip: 167°, 6° W and 359°, 8° W. In contrast, the mean of 8 attitudes measured away from the fault and the syncline is 242°, 3° NW, which is consistent with a position on the northwest flank of the Nashville dome.

Subvertical joints are exposed in the hanging wall and non-vertical joints are exposed in the footwall. Well above road level, subvertical joints extend upward from the fault, and the authors interpret these joints as fault-related tension fractures. In contrast, non-vertical joints are exposed in the footwall, and these are interpreted as zero-displacement shear fractures, because one on the north side of S.R.-840 has a strike (347°) similar to the strike of the fault and it dips 67° SW. (The rest of the joints are too high above the road to measure.) Based on physical analog experiments, Withjack et al. (1990) suggested that minor normal faults form in the footwall of a larger normal fault, because of layer parallel slip during the upward propagation of the tip of the larger normal fault, and the non-vertical joints may have formed in this way.

Because of its position west of the Harpeth River syncline and its west dip, the authors interpret the Peytonsville fault zone as a lesser structure in relation to the Arno (Stop 2) and McDaniel (Stop 4) fault zones. However, the relatively large dip separation is significant in that it underscores the relatively large amount of deformation within a couple of kilometers of the western edge of the Harpeth River syncline.

The Peytonsville fault is near the eastern edge of the Bethesda 7.5′ quadrangle (Wilson et al., 1963), although it does not appear on the map.

Stop 2. Arno Fault Zone, S.R.-840 at Arno Road Exit

(2.1 road mi east of the Peytonsville exit on S.R.-840; parking: 523577 m E, 3964836 m N, UTM Zone 16)

Take the Arno Road exit, turn left at the bottom of the off-ramp, and park under or near the 840 overpass, because parking is prohibited on off-ramps and on-ramps. Structures are exposed in roadcuts along the on-ramp for the westbound lanes (NW area) and the off-ramp for the eastbound lanes and Nathan Smith Road (SE area) as shown in Figure 7.

The Arno fault zone at Stop 2 includes the minor normal fault (AF-NW-1) having the largest dip separation (~3.8 m down-to-the-east) of any fault in the Harpeth River fault zone. The zone includes other minor faults, five mesoscale synclines, a mesoscale anticline, and both subvertical and non-vertical joints. Most of the structures are exposed within a 128-m-wide zone in the NW area. However, minor faults, non-vertical joints, and a mesoscale anticline are exposed 250 m to the southeast in the SE area. Based on the ~350° trend of most of the structures described in the following paragraphs, the SE area is structurally ENE of the NW area (Fig. 7). The authors think the NW area structures are immediately west of the western edge of the Harpeth River syncline, and that the western end of the off-ramp and the Nathan

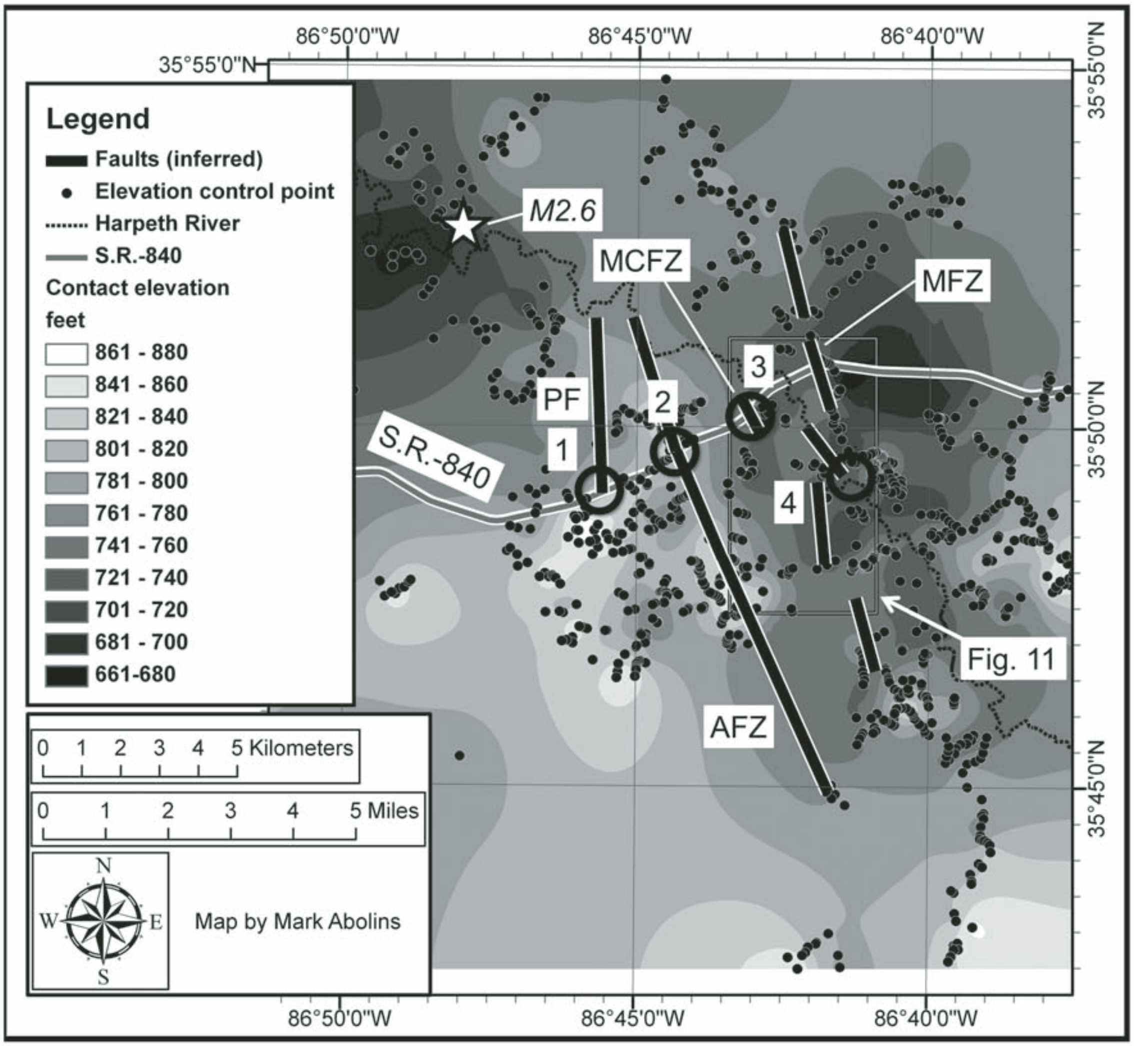

Figure 6. The location and length of inferred Harpeth River fault zone faults is based on the elevation of the contact between the Ordovician Carters Formation and the overlying Ordovician Hermitage Formation. All faults are east-side-down except for the Peytonsville fault (PF), which is west-side-down. Stops 1–4 are numbered, and the epicenter of the 8 July 2001 M2.6 earthquake is indicated. Dots indicate the location of control points for the structure contours. Geologic maps (Wilson et al., 1963; Miller and McCary, 1963) were scanned and georeferenced in ArcGIS, and control points were then digitized. Most control points are at the intersections of geologic contacts and topographic contours. Control point elevations were extracted from the National Elevation Dataset (NED). Elevations are above mean sea level. PF—Peytonsville fault; AFZ—Arno fault zone; MCFZ—McClory Creek fault zone; MFZ—McDaniel fault zone. See Figure 2 for the location of this figure in relation to the rest of the study area.

Smith Road outcrops are roughly coincident with the western edge of the Harpeth River syncline.

NW Area

The fault zone is 128 m wide along the westbound on-ramp, but all structures except for one syncline and a few subvertical joints are in the northeastern 50 m. AF-NW-1 has a strike of 344°, which is similar to the 335° strike estimated for the contact between the Ordovician Carters and Hermitage Formations from geologic maps (Fig. 6), and the fault dips 64° E. Lineations are not well developed on the fault plane, their orientation is variable, some are oblique (e.g., 118°, 49°), and few (if any) are horizontal. Where the fault penetrates thin-bedded silty carbonate, the hanging wall contains a mesoscale syncline (AS-NW-3) interpreted as a fault-related fold. The bearing of the hinge of AS-NW-3 is 349°, within 5° of the strike of the fault, but the plunge was not determined. The syncline has a kink geometry (Fig. 8), and, at its widest, the trough has a width of ~7 m along a 045° line. On the southeast side of the roadcut, the northeast limb of AS-NW-3 appears to dip up to 43° SW, and the southwest limb appears to dip up to 34° NE. Direct measurement of a bedding plane attitude at one location on the

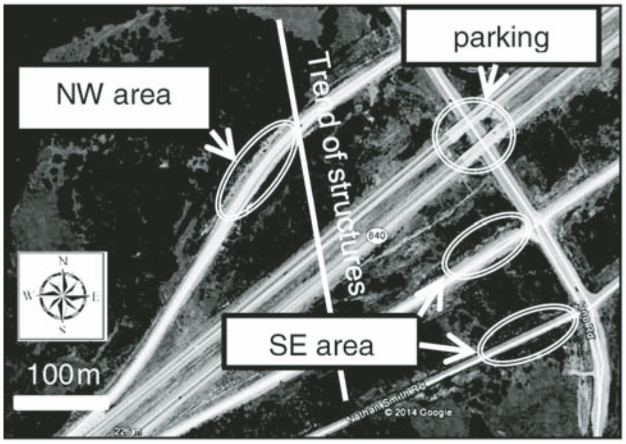

Figure 7. Location of parking and outcrops at Stop 2 (Arno Road exit on S.R.-840). The NW area is on the westbound on-ramp. The SE area includes the eastbound off-ramp and, to its southeast, Nathan Smith Road. Image from Google Earth. See Figures 2 and 6 for the location of Stop 2 in relation to the rest of the study area.

NE limb yielded 325°, 34°NE, suggesting that the roadcut is oriented at a high angle (~68°) to strike, and consequently, the true dips of the two limbs are close to the apparent dips: 45° SW and 36° NE, respectively. The dip of the northeast limb is lower on the northwest side of the roadcut. AS-NW-3 terminates upward against a detachment at the base of a relatively carbonate-rich and competent horizon, but this detachment is not visible in Figure 8.

The authors interpret AS-NW-3 as both a fault propagation fold and a fault bend fold. The authors think the southwest limb formed as a monocline above the upward propagating tip of AF-NW-1. In contrast, the NE limb may have folded in response to a shallowing of fault dip in the shallow subsurface. The NE limb is steep relative to fault bend folds formed through layer-oblique ("inclined") heterogeneous simple shear (e.g., Withjack and Schlische, 2006), suggesting the possibility that this limb could have been steepened by compressional reactivation (e.g., Marques and Nogueira, 2008) after AF-NW-1 ceased hanging-wall-down movement. Calcite strain gauge data (Craddock et al., 1993) indicates contraction in central Tennessee during Appalachian mountain-building, although no reverse or thrust faults are exposed at Stop 2. However, the steepness of the NE limb can also be explained by purely extensional layer-parallel heterogeneous simple shear, which conserves both bed length and bed thickness (e.g., Morris and Ferrill, 1999), and conjugate fractures in the footwall of AF-NW-1 are similar to those produced by layer-parallel simple shear in physical analog experiments (e.g., Withjack et al., 1990).

Other mesoscale synclines are exposed 15.3 m (AS-NW-2) and 28.7 m (AS-NW-1) northeast of AF-NW-1, and 25.5 m (AS-NW-4) and 95.5 m (AS-NW-5) southwest of AF-NW-1. With the exception of AS-NW-5, the trends of the fold hinges range from 308° to 349° (Table 1). (The trend of AS-NW-5 was not measured because it is only exposed on the north side of the on-ramp, but, because of the limited southwestern extent of outcrop on the south side of the on-ramp, the fold likely has a N, NNE, or NE bearing.) In light of the relationship between AF-NW-1 and AS-NW-3, and the similarity between the trends of the synclinal hinges and the strike of AF-NW-1, the authors hypothesize that the other four synclines are fault-related folds that formed above minor faults hidden in the shallow subsurface.

The plunges of the mesoscale synclines were not measured. However, AS-NW-1 may have a shallow NW plunge based on a best-fit axis of 334°, 4° calculated from four bedding plane measurements: 323°, 37° NE; 342°, 32° SW; 319°, 14° NE; and 337°, 25°NE.

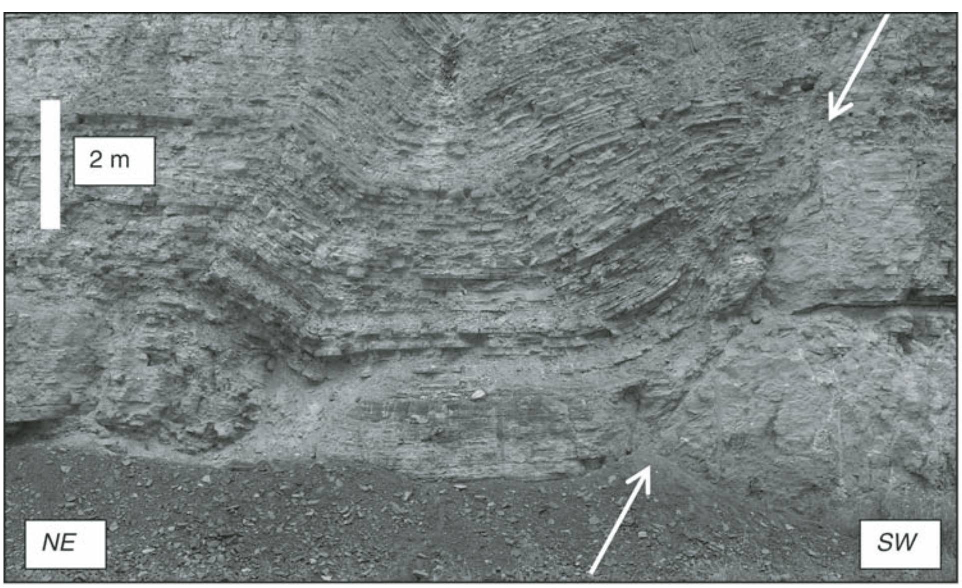

Figure 8. Mesoscale syncline in the hanging wall of minor normal fault AF-NW-1 in the NW area at Stop 2. The photo is of the southeast side of the roadcut. Arrows indicate the location of the normal fault. See Figure 7 for the location of the NW area.

TABLE 1. ORIENTATION OF FAULTS, JOINTS, AND FOLD HINGES AT STOP 2 IN THE ARNO FAULT ZONE, CENTRAL TENNESSEE

FAULTS			
Structure	Strike	Dip	Dip separation
AF-NW-1	344°	64° E	3.8 m down-to-east
AF-NW-2	327°	68° SW	30 cm down-to-west
AF-SE-1	356°	63° W	9 cm down-to-west
AF-SE-2	102°	80° N	12 cm down-to-north
JOINTS			
Structure	Strike	Dip	
J-NW-1	322°	78° NE	
J-NW-2	349°	78° NE	
J-NW-3	322°	78° NE	
J-NW-4	340°	89° NE	
J-SE-1	022°	~90°	
J-SE-2	017°	~90°	
J-SE-3	302°	66° SW	
J-SE-4	023°	62° E	
J-SE-5	345°	61° W	
J-SE-6	356°	54° E	
J-SE-7	007°	65° E	
FOLDS			
Structure	Bearing or trend	Plunge	
AS-NW-1	308°	Shallow to the NNW	
AS-NW-2	322°	Unknown	
AS-NW-3	349°	Unknown	
AS-NW-4	349°	Unknown	
AS-NW-5	Unknown	Unknown	
AA-SE-1	129°	3°	

Note: Table includes the dip separation across the faults. The designation “NW” indicates a structure in the NW area and “SE” indicates a structure in the SE area. See Figures 2 and 6 for the location of Stop 2, and see Figure 7 for the location of the NW and SE areas at Stop 2.

Where measured, the strike and dip of bedding within the synclines contrasts with the strike and dip of bedding outside the synclines. Outside the synclines, bedding plane attitudes were measured at four locations and strikes range from 198 to 242° (mean of 224°), dips ranges from 2 to 17° (mean of 6°), and dip directions are consistently northwest. Bedding plane attitudes outside the synclines are consistent with the location of Stop 2 on the northwest flank of the Nashville dome.

Minor faults and joints are exposed in several places. Moderately dipping conjugate minor faults and non-vertical joints cut thin beds of silty carbonate in the footwall of AF-NW-1 (Fig. 9) between the fault and AS-NW-4. These minor faults each have less than 5 cm of dip separation and two define a graben. Unfortunately, their strike and dip could not be measured because they are too high above the road. These conjugate faults and associated footwall graben may have formed in the same way as footwall faults in physical analog experiments (Withjack et al., 1990). Whatever their origin, conjugate faults and grabens have been observed in the footwalls of many normal faults (e.g., Jackson et al., 2006).

A minor normal fault (AF-NW-2) and subvertical joints are exposed on the northwest side of the roadcut near AS-NW-1 (Table 1). AF-NW-2 is on the southwest side of the fold, and the joints are on the northeast side. The joints are the northeasternmost structures in the NW area. Both the minor normal faults and the joints cut a medium bed of relatively pure carbonate and do not continue into overlying thin-bedded silty carbonate. The mean strike of the joints (333°) is similar to the strike of AF-NW-2, the bearing of AS-NW-2, and the best-fit bearing for AS-NW-1, so these joints are interpreted as fault related, although there is also a regional joint set striking ~300° at many central Tennessee locations.

Ball-and-pillow structures outcrop within the Hermitage Formation high on the roadcut. Holland and Patzkowsky (1997) interpreted similar structures at approximately the same horizon as seismites, and similar structures of approximately the same age have been interpreted as seismites in Kentucky and adjoining states (Pope et al., 1997; Rast et al., 1999; McLaughlin and Brett, 2004; Jewell and Ettensohn, 2004). Note, however, that some (e.g., Dineen et al., 2013) think storms have generated

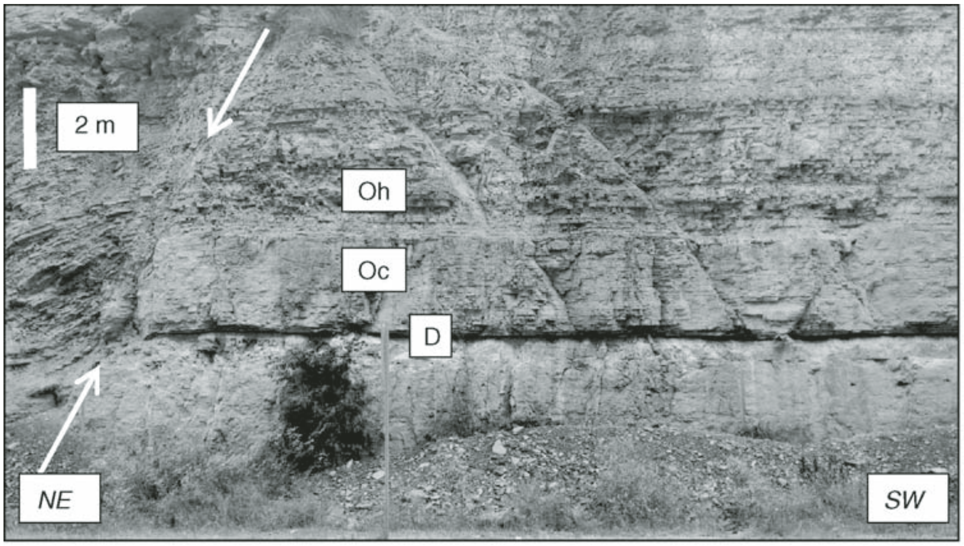

Figure 9. Mesoscale graben in the footwall of AF-NW-1 in the NW area at Stop 2. The photo is of the southeast side of the roadcut. Arrows indicate the location of the normal fault. "D" is the Deicke (T3) K-bentonite, and "Oh" and "Oc" indicate the Carters-Hermitage contact. See Figure 7 for the location of the NW area.

ball-and-pillow structures elsewhere. More soft-sediment deformation is exposed at Stop 3 and its possible significance is further discussed under Stop 3.

SE Area

Outcrops along the eastbound S.R.-840 off-ramp and along Nathan Smith Road are structurally ~150 m ENE of AF-NW-1 (Fig. 7). These outcrops generally dip east and have a strike very similar to the strike of AF-NW-1 and the bearings of AS-NW-3 and AS-NW-4, although northwest (209°, 3° NW) and southeast (244°, 3° SE) dipping strata were also measured. The mean of the east-dipping bedding plane attitudes is 349°, 7° E, and the mean of all of the bedding plane attitudes are almost the same at 350°, 5° E. The majority of bedding plane attitudes is consistent with a position on the western limb of the Harpeth River syncline, and the NW- and SE-dipping strata reflect folding parallel to the trend of the Nashville dome.

One minor fault (AF-SE-1) striking 356° and dipping 63° W was observed along the S.R.-840 off-ramp, and one minor fault (AF-SE-2) striking 103° and dipping 80° N was observed along Nathan Smith Road. AF-SE-1 has 9.5 cm of down-to-the-west dip separation across it, and AF-SE-2 has 12 cm of down-to-the-north dip separation across it. The strike of AF-SE-1 is similar to the strike of AF-NW-1, so it is likely tectonic, but the orientation of AF-SE-2 differs from the orientation of all other structures, suggesting the possibility that the fracture slipped during karstification. Five non-vertical joints (some widened into fissures by dissolution) were measured along the S.R.-840 off-ramp (Table 1). Two have strikes (302° and 023°) similar to the strikes of subvertical orthogonal joint sets widespread in central Tennessee, and the angle between the two is 86°, but the 302° joint dips 66° SW and the 023° joint dips 62° E. The authors interpret the other three (J-SE-5, J-SE-6, and J-SE-7) as fault related, because their strikes are within 23° of the strike of AF-NW-1 and the trends of AS-NW-3 and AS-NW-4. J-SE-6 is a fissure 10 cm wide and J-SE-3 is a fissure 5 cm wide. Fissuring indicates that groundwater moved along fractures near the western edge of the Harpeth River syncline.

The authors interpret the southwest end of the Nathan Smith Road outcrop and an outcrop-poor area to the west as the approximate western edge of the Harpeth River syncline. Strata dipping northwest and southeast were measured in outcrops at the southwest end of the S.R.-840 off-ramp and Nathan Smith Road, respectively, while the east-dipping strata were measured farther northeast. Near the southwest end of the Nathan Smith Road exposure, strata change orientation abruptly from 344°, 6° NE on the northeast to 244°, 3° SE on the southwest. The southeast-dipping strata may have been tilted tectonically, by karst collapse, or by both tectonic and geomorphic processes. Strata were tilted around an axis of 129°, 3°, which suggests folding because this bearing is within 1° of the bearing of AS-NW-1. Consequently, this feature is included in Table 1 as anticline AA-SE-1. Evidence of dissolution includes two subvertical dissolution fissures striking 022° (J-SE-1 on the southwest) and 017° (J-SE-2 on the northeast). These fissures are separated by ~8.1 m along a 064° bearing or 5.7 m perpendicular to the mean strike of the two fissures.

The authors think the bedrock within the outcrop-poor area likely contains fault-related fractures, and they believe the outcrop-poor area has also been the locus of much subsurface dissolution and surface erosion. Many fissures and small caves were observed and east-dipping NNW-striking joints and NE-striking subvertical joints were measured at a Nathan Smith Road outcrop (0523364 m E, 3964481 m N, UTM Zone 16) within the outcrop-poor area. Four NNW-striking joints are oriented 347°, 52° E; 341°, 60° E; 355°, 73° E; and 349°, 89 °E. These joints are interpreted as fault-related because their strike is similar to the strike of AF-NW-1 and the three non-vertical joints dip east. Other joints at the outcrop are subvertical and strike NE (025°, 026°, 027°, 031°, and 034°), which is typical of one of the

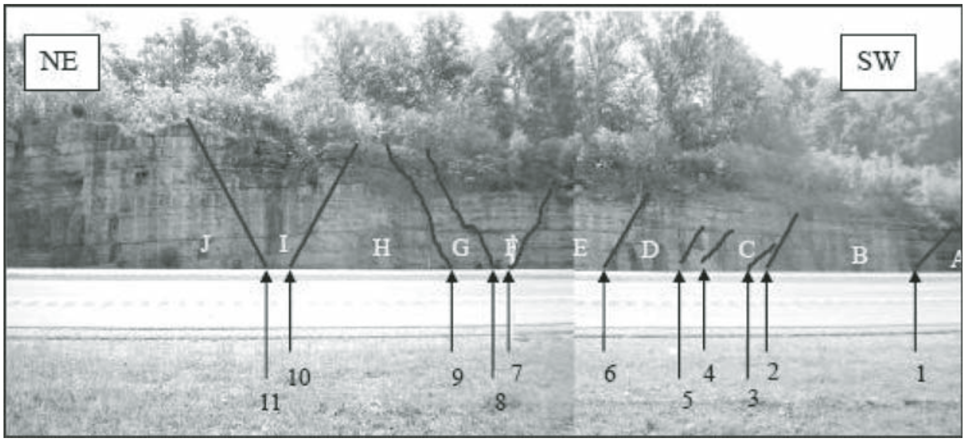

Figure 10. Minor faults in the McClory Creek fault zone at Stop 3 looking southeast. Numbers identify faults in Table 2 and letters identify places where bedding plane attitudes were measured. (Bedding plane attitudes are not listed in this chapter, but mean attitudes are described in the Stop 3 section.) See Figures 2 and 6 for the location of Stop 3 in relation to the rest of the study area.

regionally widespread joint sets. (The orientation of the outcrop biases measurements in favor of joints oriented 025–034° and against joints oriented 300°, which is the orientation of the other regionally widespread joint set.) Bedding plane attitudes measured at this location are typical of deformed parts of the NW area (005°, 5° W) and the northwest flank of the Nashville dome (258°, 5° N), but are not consistent with the western limb of the Harpeth River syncline.

The authors interpret the structures at Stop 2 as the surface expression of a blind normal fault. Based on previous geologic mapping (Fig. 6), they hypothesize that this fault has a length of ~13.2 km and is responsible for ~27 m of structural relief on the Carters-Hermitage contact. This is the longest inferred fault and it has the largest structural relief. Field observations are consistent with the size of the hypothetical fault in that AF-NW-1 has the largest dip separation of the faults described in this study, and the Arno fault zone is the widest of the Harpeth River fault zones described in this study.

The Arno fault zone is near the western edge of the College Grove 7.5′ quadrangle (Miller and McCary, 1963), although no minor faults appear on the map.

Stop 3. McClory Creek Fault Zone, S.R.-840 East of Arno Road Exit

(3.4 road mi east of the Peytonsville exit on S.R.-840; 525332 m E, 3965732 m N, UTM Zone 16)

Proceed east on S.R.-840 to mile marker 38. Park on the broad shoulder of the eastbound lanes.

After the Arno fault zone (Stop 2), the McClory Creek fault zone at Stop 3 is the best exposure of mesoscale folds and faults in central Tennessee (Fig. 10), although geologic mapping (Miller and McCary, 1963) suggests that the syncline in the hanging wall of the McClory Creek fault zone is perhaps as little as 1 km long. The relatively small dip separation (~0.9 m down-to-the-northeast) of the highest separation McClory Creek fault is consistent with the short length of the zone. Both down-to-the-northeast and down-to-the-southwest normal faults are present within the zone, but the largest dip separations are on down-to-the-northeast normal faults (Table 2). Seven northeast-side-down normal faults (1–7 in Table 2) cut gently dipping south- and southeast-dipping strata at the southwest end of the roadcut. The mean attitude of these seven normal faults is 328°, 51° NE, which is very similar to the attitudes of the two normal faults having the largest dip separations (faults 2 and 6 in Table 2). Poorly developed lineations on these two faults are roughly parallel to their dip azimuths, indicating dip slip. In addition to the normal faults, two reverse faults having apparent northeast dips and dip separations of less than 5 cm cut a thin competent bed at the southwest end of the roadcut. An anticlinal hinge bearing 121° and plunging 7° separates the southwest end of the roadcut from the northeast end. The hinge orientation is based on a best fit to six bedding plane attitudes from the southwest limb and four bedding plane attitudes from the northeast limb. A graben is coincident with the hinge, and another graben cuts gently dipping, southeast- and east-dipping strata at the northeast end of the roadcut. The three

TABLE 2. ORIENTATIONS OF AND DIP SEPARATIONS ACROSS FAULTS AT STOP 3 IN THE MCCLORY CREEK FAULT ZONE, CENTRAL TENNESSEE

Structure	Strike	Dip	Dip separation (cm)
1	309°	45° NE	11 down-to-NE
2	332°	60° NE	51 down-to-NE
3	327°	43° NE	7 down-to-NE
4	349°	48° NE	2 down-to-NE
5	296°	49° NE	5 down-to-NE
6	328°	59° NE	88 down-to-NE
7	350°	61° NE	25 down-to-NE
8	117°	66° SW	8.5 down-to-SW
9	102°	65° SW	35 down-to-SW
10	333°	63° NE	5 down-to-NE
11	110°	59° SW	1.5 down-to-SW

Note: See Figures 2 and 6 for the location of Stop 3, and see Figure 10 for the locations of the faults on the outcrop.

antithetic faults that define the northeast sides of the grabens have relatively little dip separation.

The authors interpret the minor faults and anticline at Stop 3 as the surface expression of a blind normal fault having a length of perhaps 1 km. Geologic mapping suggests that this fault is responsible for ~8 m of structural relief on the Carters-Hermitage contact (Fig. 11). The length and amount of structural relief are much less than those of the Arno fault zone.

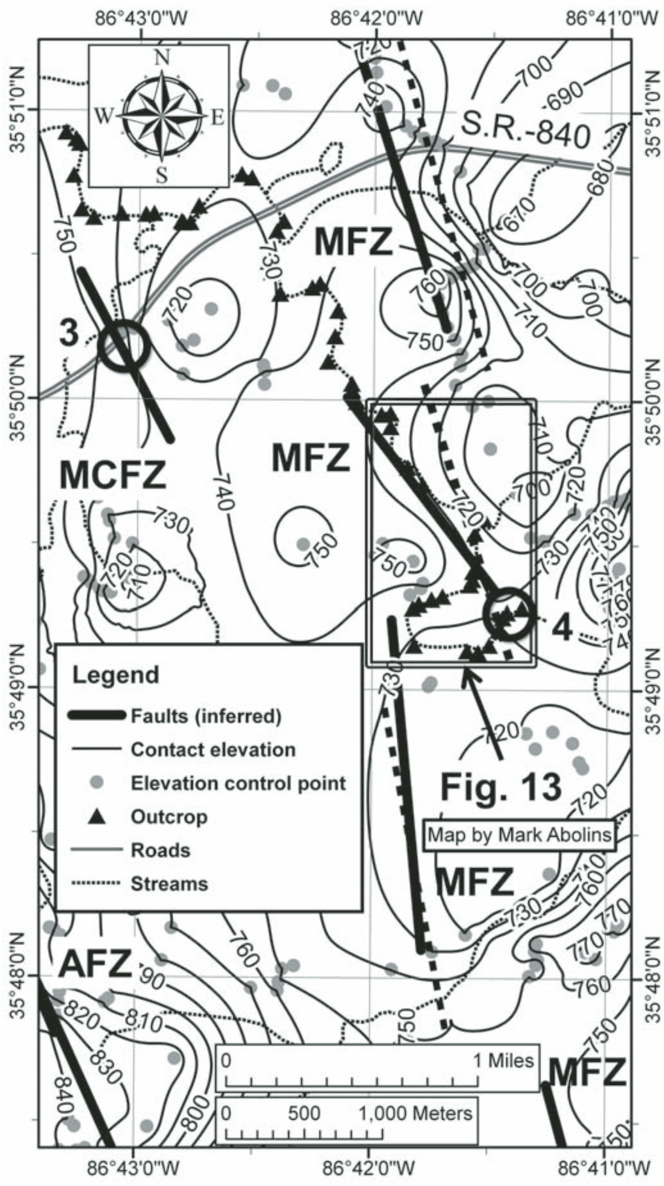

Figure 11. Elevation of the Carters-Hermitage contact relative to mean sea level. Prior to completing fieldwork, the authors mapped the McDaniel fault zone, and dotted lines show the hypothetical fault segments. At Stop 4, a karst depression and minor faults were discovered along the southeastern projection of one of the dotted lines. (See text for details.) Triangles show the locations of outcrops where no faults were found. See Figure 6 caption for sources and methods used to prepare the map. AFZ—Arno fault zone; MCFZ—McClory Creek fault zone; MFZ—McDaniel fault zone. See Figure 2 for the location of the map in relation to the rest of the study area.

Beds deformed while still soft are exposed within the Hermitage Formation at the northeast end of the roadcut well above road level. Sedimentary structures resemble illustrations of structures associated with sand volcanoes, sedimentary diapirs, and seismically induced slumps (sismoslumps) in Montenat et al. (2007). The location of these sedimentary structures within the Harpeth river fault zone and the repeated reactivation of many cratonic faults encourages consideration of the possibility that these sediments could have deformed in response to Middle Ordovician fault movements within the Nashville dome. For example, rupture of the entire length of the Arno fault zone could have generated an earthquake of approximately M6.3 based on scaling relationships in Wells and Coppersmith (1994), and an earthquake of that magnitude could have plausibly caused soft-sediment deformation (e.g., Quigley et al., 2013). However, all exposed faults in the Harpeth River fault zone are post-formational, and these sediments could have deformed in response to great earthquakes generated by faraway faults.

A fold along the eastern edge of the Harpeth River syncline is visible while driving between Stops 3 and 4. Watch for an anticline in a roadcut on the north side of S.R.-840 ~2.5 road miles east of Stop 3. The coordinates of this location are 35°50′49″N, 86°40′54″W (528740 m E, 3967007 m N, UTM Zone 16). Here, bedding plane attitudes of 159°, 5.4° W and 129°, 5.2° E define a best-fit hinge plunging 1° along a bearing of 324°. Note that Stop 4 is within the Harpeth River syncline, although part of the route between the two stops is outside the syncline.

Stop 4. McDaniel Fault Zone, the Harpeth River off Cox Road

(10.8 road mi east of the Peytonsville exit on S.R.-840; turnout and parking: 528176 m E, 3964265 m N, UTM Zone 16)

Continue east on S.R.-840 and exit onto U.S.-31A/U.S.-41A at exit 42. Turn right onto Horton Highway at the bottom of the off-ramp. After 0.6 mi, turn right onto Patton Road. After 1.8 mi (and at 9.0 road mi from the Peytonsville exit), you will see Arrington Vineyard (6211 Patton Road) on the left. This is a good place to eat a picnic lunch.

To continue on to Stop 4, drive another 0.2 mi to Cox Road and turn left. After 1.6 mi, turn right onto a farm road at 86°41′17″W, 35°49′20″ N (528176 m E, 3964265 m N, UTM Zone 16). See Figure 12 for the locations of the turnout, the karst depression, and the minor faults. Where you make the right turn, Cox Road is beginning to curve to the left and a house is visible on the left 60 m down the road. Park immediately after turning right. Walk across the railroad tracks and then walk along the boundary between the trees and field. A karst depression and the faults are at 86°41′25″, 35°49′17″N (527984 m E, 3964167 m N, UTM Zone 16). The straight-line distance between the turn off and the faults is 215 m along a bearing of 242°.

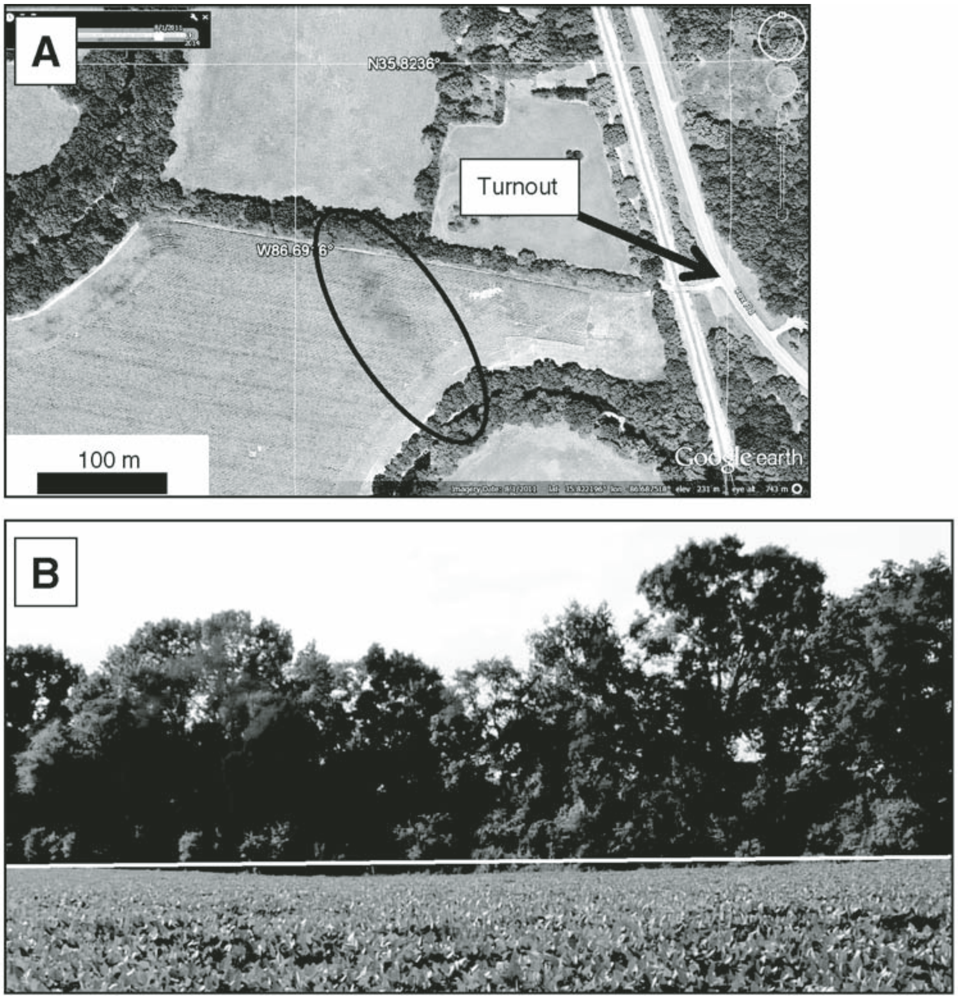

Figure 12. (A) Turnout, karst depression, and minor faults at Stop 4. The minor faults are at the southeast end of the ellipse. Image taken 1 August 2011 and obtained through Google Earth. See Figures 2 and 6 for the location of Stop 4 in relation to the rest of the study area. (B) Photo of karst depression taken from its southeastern end and looking northwest along its axis.

Geologic mapping (Figs. 6 and 11) suggests that the McDaniel fault zone is almost as long (11.6 km) and is responsible for almost as much structural relief (24 m) as the Arno fault zone, but it is not exposed in any roadcuts. Two of the authors (Abolins and Camacho) found four minor faults along the southeastern projection of one segment of the zone where the McDaniel fault zone intersects the Harpeth River. At this location, the zone is ~50 m wide and consists of three northeast-side-down normal faults and one southwest-side-down normal fault (Table 3). The SW-dipping normal fault and one of the NE-dipping normal faults define a graben between 10 and 15 m from the NE end of the zone. All of the minor faults have less than 1 m of dip separation across them.

TABLE 3. ORIENTATIONS OF AND DIP SEPARATIONS ACROSS FAULTS AT STOP 4 IN THE MCDANIEL FAULT ZONE, CENTRAL TENNESSEE

Structure	Strike	Dip	Dip separation (cm)
MFZ-1	297°	~90°	<50 cm down-to-NE
MFZ-2	312°	74° SW	~35 cm down-to-SW
MFZ-3	318°	85° NE	50–90 cm down-to-NE
MFZ-4	320°	78° NE	~30 cm down-to-NE

Note: See Figures 2 and 12 for the location of Stop 4.

The strata are fissured and collapse related to karstification has overprinted tectonic structures at this location. Indeed, the agricultural field immediately northwest of Stop 4 contains a depression interpreted as a karst feature (Fig. 12). This depression is elongate along the strike of the minor normal faults, is on projection with them, and drains to the river where the northeasternmost fault outcrops.

As shown in Figures 13 and 14, the authors interpret the minor normal faults at Stop 4 as the southeastern termination of one segment of the McDaniel fault zone. To the south, the fault zone steps to the west. The authors interpret the entire fault zone as the surface manifestation of a blind normal fault.

The McDaniel fault zone segment northwest of Stop 4 is coincident with a lineament mapped by Reesman and Stearns (1985).

Gently northwest-dipping strata of the Nashville dome are visible on the drive between Stops 4 and 5. Between 1.5 and 3.1 road mi east of the intersection between S.R.-840 and Horton Highway (Exit 42), bedding plane attitudes of 241°, 2° NW and 255°, 3° NW were measured in roadcuts on the NW side of

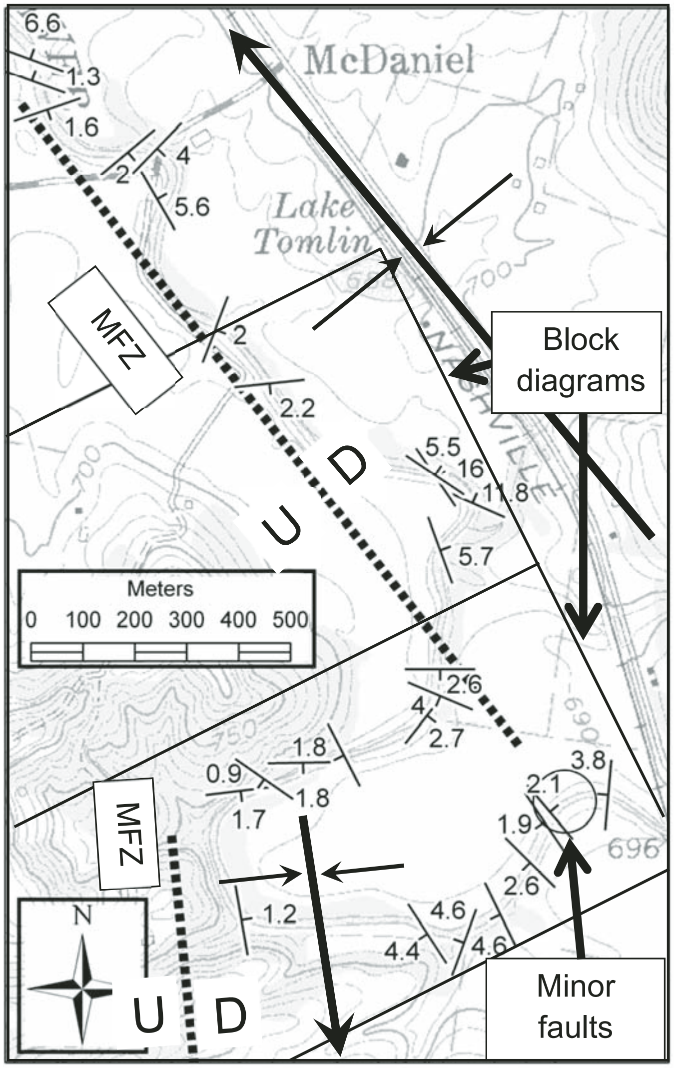

Figure 13. Interpretation of minor faults at Stop 4 as the southeastern termination of a fault segment within the McDaniel fault zone. To the south, the fault zone steps to the west. See Figure 11 for the location of the map in relation to the rest of the study area.

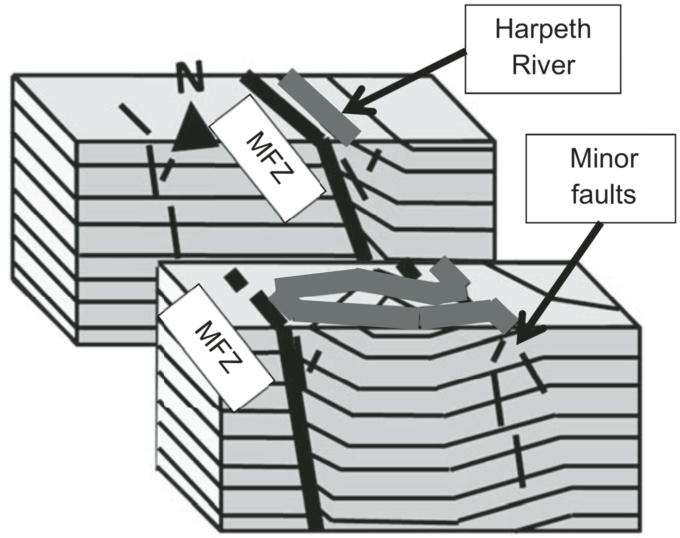

Figure 14. Block diagrams depicting the interpretation of minor faults at Stop 4 as the southeastern termination of a fault segment within the McDaniel fault zone (MFZ). See Figure 13 for the location of the block diagrams and the geology on which they are based.

S.R.-840 at 35°50′30″N, 86°38′9″W (532883 m E, 3966444 m N, UTM Zone 16) and 35°51′9″N, 86°36′40″W (535126 m E, 3967645 m N, UTM Zone 16).

Stop 5. Western Edge of the Stones River Syncline, West Bank of the West Fork of the Stones River at Nice Mill Dam

(31.3 road mi from the Peytonsville exit on S.R.-840; parking: 548125 m E, 3977452 m N, UTM Zone 16)

Turn left onto Cox Road, drive 1.6 mi, and then turn right onto Patton Road. Drive 2.0 mi and turn left onto Horton Highway. After 0.6 mi, get on S.R.-840 going east toward Murfreesboro. After 14.9 mi, exit at Sulfur Springs Road (Exit 57). Drive 0.3 mi to the top of the off-ramp and turn left onto Sulfur Springs Road. After a little more than 1.4 mi, pass a parking area and then cross over the West Fork of the Stones River. Immediately after crossing over the river, make a hard right into the west bank parking area for Nice Mill Dam Recreation Area.

This stop is above the hypothetical Stones River fault zone. The fault zone hypothesis is largely based on the relationship between the Harpeth River syncline and faults in the Harpeth River fault zone. As in the Harpeth River fault zone, there is a syncline with an axis trending NNW and N (Moore et al., 1969), and Galloway (1919) mapped a minor fault at a location (now beneath Percy Priest Reservoir) along the western edge of the syncline. In addition, Wilson (1964) mapped another minor fault nearby. The syncline and hypothetical fault are shown in Figure 15. The description of this stop and the description of Stop 6 present preliminary evidence supporting the existence of the Stones River fault zone. No minor normal faults are exposed at this stop, but joints and bedding were measured on the west bank of the Stones River at Nice Mill Dam and at a second location 300 m to the northeast on the east bank.

The west bank location is west of the Stones River syncline because no strata dip east. The authors think the geology and structural position of this stop may be similar to that of Stop 2 at the southwestern end of the Nathan Smith Road exposures in the SE area (Fig. 7). At the west bank location, ESE-dipping joints (NJS-W-1) cut an anticline with a hinge bearing 342° and plunging 4°. The hinge of the anticline is based on three bedding plane attitudes from the NE limb of the fold (NB-W-1 through NB-W-3 in Table 4) and three bedding plane attitudes from the SW limb of the fold (NB-W-7 through NB-W-9). The other attitudes (NB-W-4 through NB-W-6) are interpreted as hinge attitudes. The mean attitude for the NE limb is 258°, 4° N and the mean attitude for the SW limb is 191°, 7° W; the intersection of the two means provides the hinge orientation.

Measurement of 29 joints at the west bank location revealed two possible joint sets in addition to the regional joints common in central Tennessee (Fig. 16A), although more measurements are needed to confirm the presence of these sets. The strike of joint set NJS-W-1 ranges from 334° to 001°, the dip ranges from 57° to 88° E, and the mean strike and dip (n = 12) are 344° and

TABLE 4. ORIENTATIONS OF BEDDING ON THE WEST BANK OF THE WEST FORK OF THE STONES RIVER AT STOP 5 IN THE STONES RIVER FAULT ZONE

Station	Strike	Dip	Position on fold
NB-W-1	256°	5.3° N	NE limb
NB-W-2	256°	0.5° N	NE limb
NB-W-3	261°	4.8° N	NE limb
NB-W-4	208°	3.2° NW	Hinge
NB-W-5	224°	5.6° NW	Hinge
NB-W-6	161°	5.7° SW	Hinge?
NB-W-7	188°	9.7° W	SW limb
NB-W-8	194°	11.1° W	SW limb
NB-W-9	181°	1.2° W	SW limb

Note: See Figures 2 and 15 for the location of Stop 5.

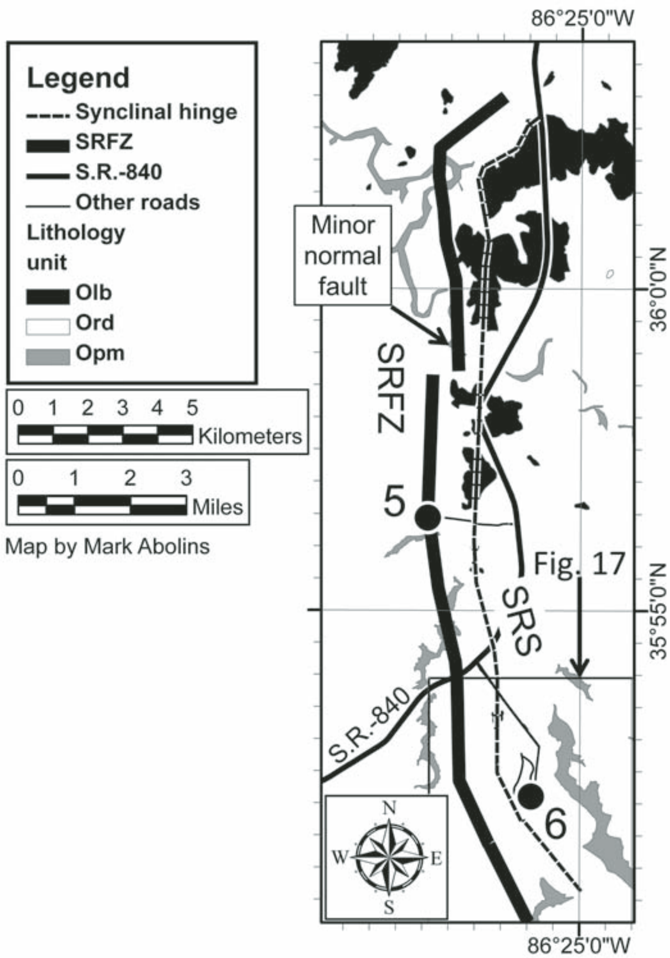

Figure 15. The Stones River syncline (SRS) and the hypothetical Stones River fault zone (SRFZ). The Stones River syncline is defined by a roughly N-S belt of the relatively young Ordovician Lebanon limestone (Galloway, 1919; Wilson and Hughes, 1963; Wilson, 1964). The Lebanon limestone is flanked by the older Pierce and Murfreesboro limestones, and their outcrop pattern has been taken from Wilson (1964, 1965) and Wilson and Hughes (1963). Note, however, that subsurface investigations in the southern part of the area shown on the figure (Farmer and Hollyday, 1999), and surface investigations farther south (Abolins, 2014) have shown that the Pierce and Murfreesboro outcrops pattern is not accurately depicted by one or more of the existing geologic maps at many locations. See Figure 2 for the location of this figure relative to the rest of the study area. Olb—Ordovician Lebanon limestone; Ord—Ordovician Ridley limestone; Opm—Ordovician Pierce limestone.

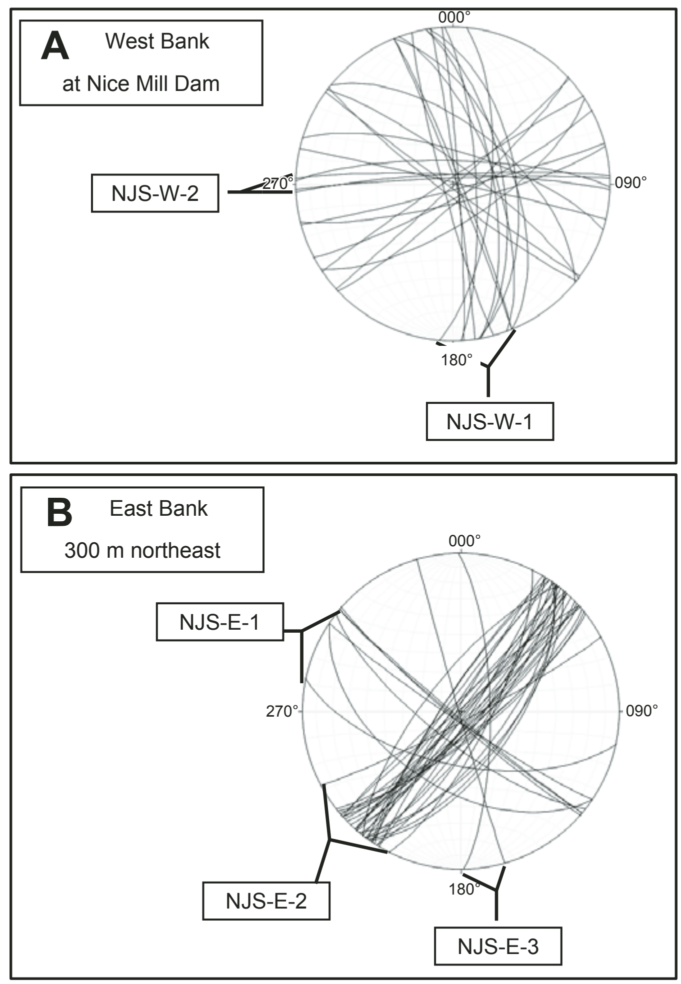

Figure 16. Joint orientations at and near Stop 5. (A) Orientation of joints on the west bank of the West Fork of the Stones River at Nice Mill Dam, including two possible sets that are not widespread in central Tennessee. (B) Orientation of joints 300 m northeast of Nice Mill Dam, including two sets (NJS-E-1 and NJS-E-2) that are widespread and two joints (NJS-E-3) having an orientation falling within the range of orientations observed for NJS-W-1 on the west bank. See Figure 15 for the location of Stop 5 within the SRFZ.

76° E, respectively. The mean strike of this set is similar to the bearing of the anticlinal hinge, the strike of the hypothetical Stones River fault zone, and the strike of minor faults in the Harpeth River Fault Zone. For these reasons and because the joints are consistently east-dipping and coincide with an anticline, the authors interpret these joints as fault related. The strike of possible joint set NJS-W-2 ranges from 263° to 268 °, the dip ranges from 78° to 87° N, and the mean strike and dip (*n* = 4) are 266° and 84° N, respectively. The strike of NJS-W-2 is similar to the strike of the NE limb of the fold.

The joint orientations on the west bank at Nice Mill Dam contrast with those at a location on the east bank of the Stones River 300 m to the northeast (Fig. 16B). That location is within the west limb of the Stones River syncline, because the mean of seven bedding plane attitudes is 325°, 6° E. The 44 joint orientations measured on the east bank were for the most part typical of central Tennessee. The most prominent set (NJS-E-2) has a strike ranging from 023 to 058° and a mean strike and dip of 037° and 84° E, respectively. The other possible set (NJS-E-1) has a strike ranging from 278 to 307° and a mean strike and dip of 301° and 76° SW, respectively. The relatively small number of joints in this set likely reflects sampling bias, because the mean strike of the set is similar to the trend of the cliff where measurements were made. The relatively shallow mean dip is unusual, but only six joints were measured and one having a dip of 50° pulled down the mean. At the east bank location, only two joints (NJS-E-3) had strikes placing them within the range of NJS-W-1 and no joint strikes fell within the range of NJS-W-2.

Stop 6. Near the Hinge of the Stones River Syncline, the Slaughter Pen, Stones River National Battlefield

(38.5 road mi from the Peytonsville exit off Thompson Lane; parking: 551376 m E, 3969598 m N)

Turn left onto Sulfur Springs Road. After 1.6 mi, get on S.R.-840 going west. After 2.2 mi, take Exit 55A for 41/70S

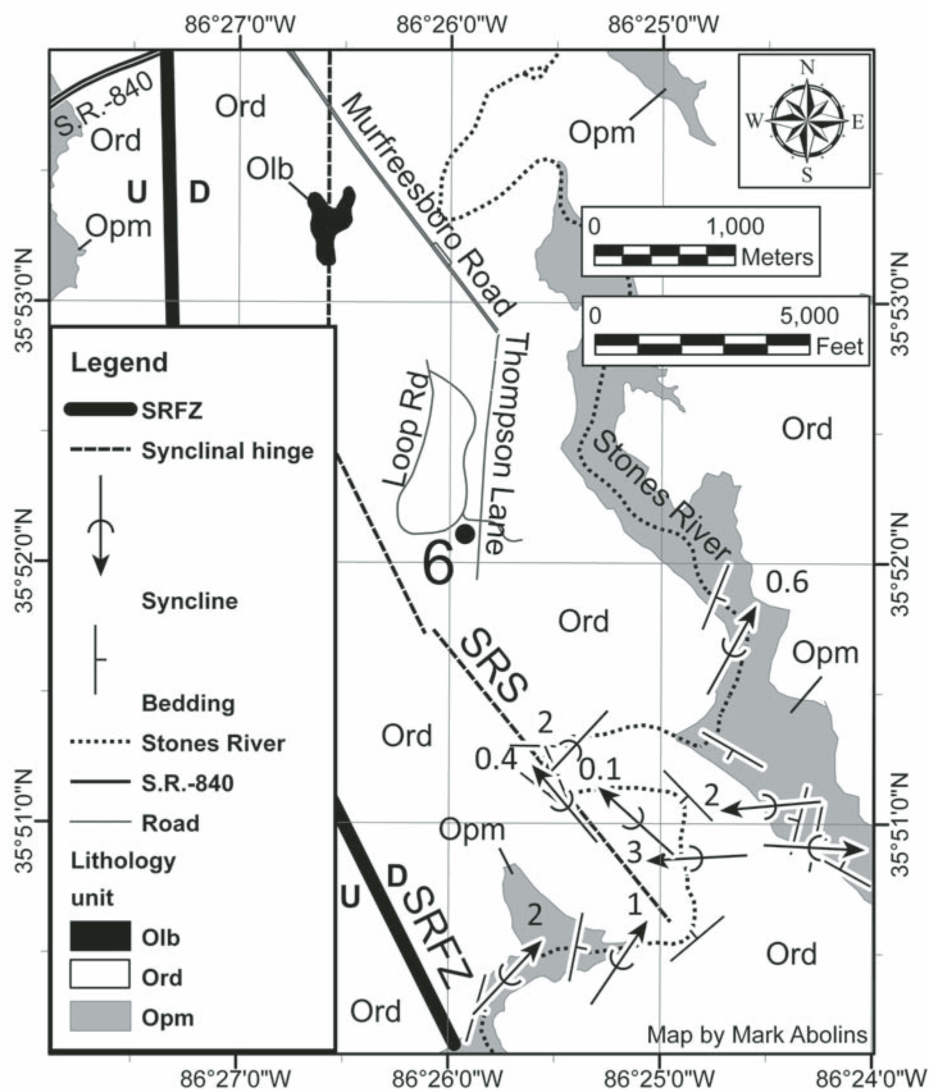

Figure 17. Geology of the Stones River syncline (SRS) and Stones River fault zone (SRFZ) in the vicinity of Stop 6. The outcrop pattern of the Lebanon limestone constrains the Stones River syncline hinge to the northwest of Stop 6, and bedding plane attitudes constrain the location of the hinge to the south. All attitudes are the mean of at least six measurements. Dip values have been omitted for clarity. Fold hinge orientations are from the intersection of adjacent bedding plane attitudes. On the limbs of the syncline, high-order folds plunge toward the syncline hinge, and, near the hinge, high-order folds have hinges parallel to the hinge of the syncline. See the Figure 15 caption for a caveat about the outcrop pattern of the Pierce and Murfreesboro limestones. See Figure 2 for the location of this figure relative to the rest of the study area. Olb—Ordovician Lebanon limestone; Ord—Ordovician Ridley limestone; Opm—Ordovician Pierce limestone.

Murfreesboro Road and get on Murfreesboro Road going toward Murfreesboro. After going 2.0 mi on Murfreesboro Road, turn right onto Thompson Lane. Continue for 0.6 mi on Thompson Lane. Turn right into Stones River National Battlefield. Go 0.2 mi and park at the Slaughter Pen.

The Slaughter Pen is a fissured and forested area where Union troops fought a bloody defensive action on the morning of 31 December 1862 during the Battle of Stones River (e.g., McDonough, 1989; Daniel, 2012). Previous geologic mapping (Figs. 15 and 17) suggests that the Slaughter Pen is within the Stones River syncline ~600 m northeast of the hinge. Based on observations described below, the authors think the Slaughter Pen is in the hinge of a parasitic fold and that fissures are fold-related.

The authors measured 37 bedding plane attitudes and found that almost all poles to bedding plunge southwest, south, or southeast with many plunging south and indicating a mean bedding plane attitude of 274°, 3° N (Fig. 18A). Given the location of Stop 6 within and east of the Stones River syncline hinge, W, SW, or NW dips would be expected. The most plausible explanation for the N dip of bedding is that Stop 6 is on the hinge of a fold parasitic to the syncline and having a hinge bearing ~004° and plunging 3°. The N plunge of the parasitic fold hinge is similar to the N plunge of the Stones River syncline hinge ~1.1 km to the NW.

Field observations indicate a master joint set (SJS-1) and a cross joint set (SJS-2) as shown in Figure 18B. Students from the Middle Tennessee State University (MTSU) Fall 2014 Field Methods in Geology course measured the strike of 109 subvertical fissures (joints) along 15 30-m traverses. The trend of eight traverses was 080° and the trend of seven traverses was 350°. Because of the sampling technique, they obtained a relatively unbiased data set, although fissures having orientations close to 080° should be under-represented by 88% relative to those striking ~350°. Also, fissures striking ~035° and 305° should be over-represented by 133%, all else being equal. They found that SJS-1 has a mode of 350–355° (Fig. 18B), which is within 9–14° of the bearing of the inferred fold hinge. Consequently, these joints are thought to have formed during folding and through extension perpendicular to the hinge. Cross joints (SJS-2) have a mode of 085–090°, which is approximately orthogonal to the strike of SJS-1. At this stop, few joints belong to the regionally widespread sets NJS-E-1 and NJS-E-2 observed east of Nice Mill Dam (Fig. 16) and at many other central Tennessee locations.

Groundwater flow through SJS-1 cannot solely explain groundwater flow paths (Fig. 3) in the vicinity of Stop 6, because dye traces show water flowing in a more northwesterly direction. The northwest flow paths require considerable flow through other joints (e.g., SJS-2) in addition to flow through SJS-1. However, a belt of 341–020° dye traces begins ~1.9 km NW of the Slaughter Pen and extends for ~6 km to the NNW. Flow through SJS-1, NJS-W-1 or both explains the 341–020° flow paths.

DISCUSSION AND CONCLUSIONS

The stops described in this field guide provide an opportunity to explore the connection between mesoscale faults, joints, and folds observed in outcrop and macroscale faults and folds inferred from existing geologic maps (Figs. 6, 11, and 15). As described under the road guide entries for Stops 1–4, many mesoscale structures likely formed in response to slip on blind basement normal faults as conceptualized in Figure 1. Table 5 summarizes the characteristics of these faults. Observations along S.R.-840 suggest that physical analog models of normal

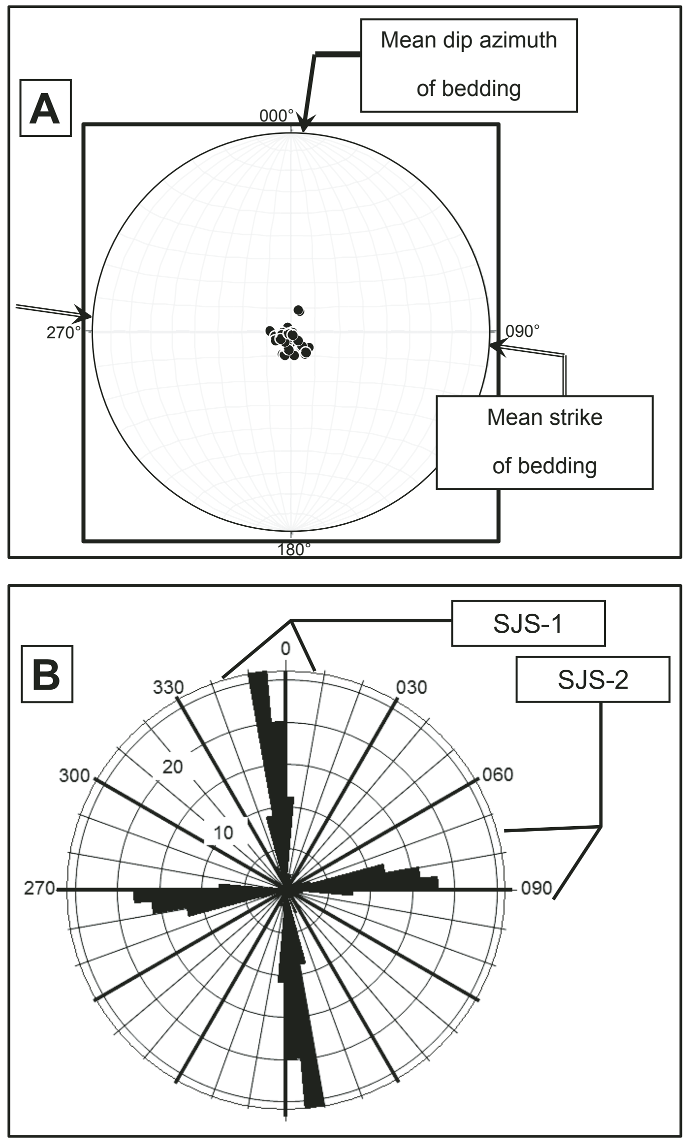

Figure 18. Bedding plane and joint orientations at Stop 6. (A) Poles to bedding planes and the strike and dip azimuth of the plane orthogonal to the mean pole. (B) Joint orientations, indicating at least two sets: SJS-1 and SJS-2. See Figures 2 and 15 for the location of Stop 6 in relation to the rest of the study area.

TABLE 5. CHARACTERISTICS OF THE HARPETH RIVER AND STONES RIVER FAULT ZONES

Fault zone	Strike	Shear sense	Length (km)	Max. structural relief (m)	Max. dip separation on a minor fault (m)
Peytonsville	358°	West down	4.7	10?	1.1
Arno	350°	East down	13.2	27	3.8
McClory Creek	331°	East down	1	8	0.9
McDaniel	340°	East down	11.6	24	<1
Stones River	356°	East down	25	40? (approximate thickness of Ridley limestone)	Unknown

Note: See Figure 2 for locations of the faults.

faulting (Withjack et al., 1990) and field studies of rifts (e.g., Jackson et al., 2006) and extended regions (e.g., Berg and Skar, 2005) are relevant to understanding cratonic faults and folds in central Tennessee.

The Importance of Field Geology and Geologic Maps

This chapter shows how field geology reveals hypothetical basement faults missed by most geophysical techniques. The faults inferred here do not appear on the Sims et al. (2008) or Johnson et al. (1994) maps, which are largely based on magnetics and microgravity. Indeed, faults responsible for less than 50 m of dip separation on the basement-cover contact should be difficult to detect with microgravity given the low-density contrast between compacted carbonate sedimentary rock and granite. Stearns and Reesman (1986) used magnetics to infer a greater depth to magnetic basement beneath the Harpeth River syncline. However, they thought the reliability of their analysis was limited, and they did not infer the locations of specific faults.

This paper underscores the importance of using geologic maps to discover surface exposures of minor faults. Specifically, this chapter contains a good example of the use of a geologic map and an air photo to discover minor faults and a karst feature at Stop 4. The authors used a geologic map (Miller and McCary, 1963) to make a structure contour map, and then used the structure contour map to predict the location of segments of the McDaniel fault zone (dotted lines on Fig. 11) even though the fault zone is not exposed in roadcuts. Then, two of the authors (Abolins and Camacho) searched the banks of the Harpeth River, finding four minor normal faults within a 50-m-wide zone along the southeastern projection of one fault segment. In contrast, Abolins and Camacho found no other faults during the examination of 84 outcrops along 13.3 km of the Harpeth River. After discovering the minor faults, examination of a 1 August 2011 Google Earth air photo revealed a dark elliptical feature extending northwest from the minor faults and having a long axis parallel to the strike of the faults (Fig. 12A). Subsequently, field examination of the feature showed that it is a karst depression (Fig. 12B) draining into the fault zone.

Additionally, this paper underscores the importance of using geologic maps to understand the significance of mesoscale structures exposed in roadcuts. For example, numerous faults, folds, and joints are exposed at both Stops 2 and 3. However, examination of structure contour maps (Figs. 6 and 11) shows that Stop 2 likely sits atop the 13.2-km-long Arno fault, which is responsible for up to 27 m of structural relief, while the inferred McClory Creek fault below Stop 3 is likely as short as 1 km and is responsible for as little as 8 m of structural relief.

Tectonic Significance

The findings in this chapter are consistent with suggestions by Marshak and Paulsen (1996) and Marshak et al. (2000) that many Paleozoic uplifts formed in places where the crust extended during the Proterozoic (or earliest Cambrian), and, specifically, that the Nashville dome coincides with a Precambrian rift (Liang and Langston, 2009). However, the nature of extensional structures in the basement remains largely unknown. Was central Tennessee the site of a rift, or was it the site of a few normal faults on the periphery of more strongly extended areas like the Reelfoot rift (e.g., Csontos et al., 2008)?

ACKNOWLEDGMENTS

This research was supported by Research Experience for Undergraduates (REU) grant NSF-EAR1263238 to Mark Abolins and Heather Brown, a Middle Tennessee State University (MTSU) Faculty Research and Creative Activity Grant to Abolins, and MTSU Undergraduate Research and Creative Activity (URECA) grants to Mark Trexler, Alex Ward, and Rachel Forlines. Matt Cooley was supported by NSF-DUE0431652 to Tom Cheatham and co-investigators. MTSU undergraduates Jason Pomeroy and Kyle Wiseman were also supported by the NSF-DUE grant, and they worked with Cooley on the geology depicted in Figure 17. Brandi Bomar and Indya Evans (NSF REU summer 2014 participants) and Rachel Forlines contributed to discussions about the geology described in this study, and they contributed to the preparation of Figure 15. Amanda Brown and Emily Silveira (NSF REU summer 2013 participants) helped make structural measurements in the SE area at Stop 2. MTSU undergraduate Michael Copley helped with field logistics during collection of data for Stop 5.

The Fall 2014 MTSU Field Methods in Geology students verified structural measurements at Stops 2 and 3, and they made the fissure orientation measurements shown in Fig. 18B and described in the accompanying text.

MTSU colleagues Clay Harris and Ron Zawislak contributed greatly to this work through numerous discussions over many years.

The manuscript benefited from reviews by Randy Cox, Charles Trupe, and Ann Holmes, although they may not agree with all of the interpretations and conclusions.

REFERENCES CITED

Abolins, M.J., 2014, Undergraduates discovering folds in "flat" strata: An unusual undergraduate geology field methods course: Journal of Geoscience Education, v. 62, p. 264–277, doi:10.5408/12-371.1.

Beaumont, C., Quinlan, G., and Hamilton, J., 1988, Orogeny and stratigraphy: Numerical models of the Paleozoic in the eastern interior of North America: Tectonics, v. 7, p. 389–416, doi:10.1029/TC007i003p00389.

Berg, S., and Skar, T., 2005, Controls on damage zone asymmetry of a normal fault zone: Outcrop analyses of a segment of the Moab fault, SE Utah: Journal of Structural Geology, v. 27, p. 1803–1822, doi:10.1016/j.jsg.2005.04.012.

Bordine, B.W., 1977, Right lateral fault and associated karst features, Northeast Rutherford County, Tennessee: Tennessee Academy of Sciences, v. 52, p. 67–68.

Craddock, J.P., Jackson, M., van der Pluijm, B.A., and Versical, R.T., 1993, Regional shortening fabrics in eastern North America: Far-field stress transmission from the Appalachian-Ouachita orogenic belt: Tectonics, v. 12, p. 257–264, doi:10.1029/92TC01106.

Crawford, N.C., 1988, Karst Hydrology Investigation in the Vicinity of the Campus-Injector Complex for the Proposed Middle Tennessee Site for the Superconducting Super Collider: Nashville, Tennessee Division of Geology, 27 p., 7 plates.

Csontos, R., Van Arsdale, R., Cox, R., and Waldron, B., 2008, Reelfoot rift and its impact on Quaternary deformation in the central Mississippi River valley: Geosphere, v. 4, p. 145–158, doi:10.1130/GES00107.1.

Daniel, L.J., 2012, Battle of Stones River: The Forgotten Conflict between the Confederate Army of Tennessee and the Union Army of the Cumberland: Baton Rouge, Louisiana State University Press, 313 p.

Dineen, A.A., Fraiser, M.L., and Isbell, J.L., 2013, Palaeoecology and sedimentology of Carboniferous glacial and post-glacial successions in the Paganzo and Rio Blanco basins of northwestern Argentina, *in* Gasiewicz, A., and Stowakiewicz, M., eds., Paleozoic Climate Cycles: Their Evolutionary and Sedimentological Impact: Geological Society, London, Special Publication 376, p. 109–140.

Farmer, J.J., and Hollyday, E.F.P., 1999, Regional Subsurface Correlation of the Pierce Limestone and Adjacent Limestones of Middle Tennessee: U.S. Geological Survey Report of Investigations 47, 21 p.

Fisher, C.M., Loewy, S.L., Miller, C.F., Berquist, P., Van Schmus, W.R., Hatcher, R.D., Jr., Wooden, J.L., and Fullagar, P.D., 2010, Whole-rock Pb and Sm-Nd isotopic constraints on the growth of southeastern Laurentia during Grenvillian orogenesis: Geological Society of America Bulletin, v. 122, p. 1646–1659, doi:10.1130/B30116.1.

Galloway, J.J., 1919, Geology and Natural Resources of Rutherford County, Tennessee: Nashville, Tennessee Division of Geology Bulletin 22, 81 p.

Holland, S., and Patzkowsky, M., 1997, Distal orogenic effects of peripheral bulge sedimentation: Middle and Upper Ordovician of the Nashville dome: Journal of Sedimentary Research, v. 67, p. 250–263.

Jackson, C.A.L., Gawthorpe, R.L., and Sharp, I.R., 2006, Style and sequence of deformation during extensional fault-propagation folding: Examples from the Hammam Faraun and El-Qaa fault blocks, Suez Rift, Egypt: Journal of Structural Geology, v. 28, p. 519–535, doi:10.1016/j.jsg.2005.11.009.

Jewell, H.E., and Ettensohn, F.R., 2004, An ancient seismite response to Taconic far-field forces: The Cane Run Bed, Upper Ordovician (Trenton) Lexington Limestone, Central Kentucky (USA): Journal of Geodynamics, v. 37, p. 487–511, doi:10.1016/j.jog.2004.02.017.

Johnson, P.R., Zietz, I., and Thomas, W.A., 1994, Possible Neoproterozoic–early Paleozoic grabens in Mississippi, Alabama, and Tennessee: Geology, v. 22, p. 11–14, doi:10.1130/0091-7613(1994)022<0011:PNEPGI>2.3.CO;2.

Kunk, M.J., and Sutter, J.F., 1984, ^{40}Ar/^{39}Ar age spectrum dating of biotite from Middle Ordovician bentonites in Eastern North America, *in* Bruton, D.L., ed., Aspects of the Ordovician System: Oslo, Norway, University of Oslo, Paleontologisk Museum, Paleontological Contributions from the University of Oslo, no. 295, p. 11–22.

Liang, C., and Langston, C.A., 2009, Three-dimensional crustal structure of eastern North America extracted from ambient noise: Journal of Geophysical Research, v. 114, B03310, doi:10.1029/2008JB005919.

Mallory, M.J., 1974, Bouguer gravity map and a postulated basement structure configuration of the Nashville West and Oak Hill Quadrangles, Tennessee [M.S. thesis]: Nashville, Vanderbilt University, 47 p.

Marques, F.O., and Nogueira, C.R., 2008, Normal fault inversion by orthogonal compression: Sandbox experiments with weak faults: Journal of Structural Geology, v. 30, p. 761–766, doi:10.1016/j.jsg.2008.02.015.

Marshak, S., and Paulsen, T., 1996, Midcontinent U.S. fault and fold zones: A legacy of Proterozoic intracratonic extensional tectonism?: Geology, v. 24, p. 151–154, doi:10.1130/0091-7613(1996)024<0151:MUSFAF>2.3.CO;2.

Marshak, S., Karlstrom, K.E., and Timmons, J.M., 2000, Inversion of Proterozoic extensional faults: An explanation for the pattern of Laramide and ancestral Rockies intracratonic deformation, United States: Geology, v. 28, p. 735–738, doi:10.1130/0091-7613(2000)28<735:IOPEFA>2.0.CO;2.

Matthews, L.E., 1971, A study of the structure of the Ridley Limestone in the Gladeville Quadrangle in central Tennessee [M.S. thesis]: Nashville, Vanderbilt University, 76 p.

McDonough, J.L., 1989, Battle of Stones River, *in* McPherson, J.M., ed., Battle Chronicles of the Civil War: 1862: Middlebury, Connecticut, Grey Castle Press, p. 286–320.

McLaughlin, P.I., and Brett, C.E., 2004, Eustatic and tectonic control on the distribution of marine seismites: Examples from the Upper Ordovician of Kentucky, USA: Sedimentary Geology, v. 168, p. 165–192.

Miller, R., and McCary, C., 1963, Geologic Map and Mineral Resources Summary of the College Grove Quadrangle: Tennessee Division of Geology Geologic Quadrangle Map 70-SW, 1:24,000 scale.

Min, K., Renne, P.R., and Huff, W.D., 2001, ^{40}Ar/^{39}Ar dating of Ordovician K-bentonites in Laurentia and Baltoscandia: Earth and Planetary Science Letters, v. 185, p. 121–134, doi:10.1016/S0012-821X(00)00365-4.

Montenat, C., Barrier, P., d'Estevou, P.O., and Hibsch, C., 2007, Seismites: An attempt at critical analysis and classification: Sedimentary Geology, v. 196, p. 5–30, doi:10.1016/j.sedgeo.2006.08.004.

Moore, G.K., Burchett, C.R., and Bingham, R.H., 1969, Limestone Hydrology in the Upper Stones River Basin, Central Tennessee: Nashville, Tennessee Department of Conservation, Division of Water Resources, 58 p.

Morris, A.P., and Ferrill, D.A., 1999, Constant-thickness deformation above curved normal faults: Journal of Structural Geology, v. 21, p. 67–83, doi:10.1016/S0191-8141(98)00098-4.

Ogden, A.E., and Powell, B.E., 1999, Ground water spring basin delineation in Rutherford Co., TN for interpreting sinkhole flooding—Year two: Results of the investigation, *in* Proceedings, Tennessee Water Resources Symposium, 9th: Nashville, Tennessee, American Water Resource Association, p. 1B-5–1B-16.

Ogden, A.E., and Scott, A.T., 1998, Delineation of ground water spring basins in Rutherford Co., TN: A first step in understanding sinkhole flooding, *in* Proceedings, Tennessee Water Resources Symposium, 9th: Nashville, Tennessee, American Water Resource Association, p. 2B-7–2B-17.

Ogden, A.E., Hays, K.H., and Storvik, P., 1998, Ground water tracing results at the Murfreesboro Old City Dump in Rutherford Co. TN, *in* Proceedings, Tennessee Water Resources Symposium, 8th: Nashville, Tennessee, American Water Resource Association, p. 1B-29–1B-38.

Ogden, A.E., Ogden, L.R., Godfrey, A., Wright, A., and Storvik, P., 1999, Ground water tracing results at the Rosebank Dump, Rutherford Co, TN, *in* Proceedings, Tennessee Water Resources Symposium, 9th: Nashville, Tennessee, American Water Resource Association, p.1B-19–1B-29.

Ogden, A.E., Ogden, L.R., and Powell, B.E., 2001, An inventory of Class V Injection wells (sinkholes) in Rutherford County with ground water tracing results, *in* Proceedings, Tennessee Water Resources Symposium, 11th: Nashville, Tennessee, American Water Resource Association, p. 3B-8–3B-14.

Ogden, A.E., James, R., Ketner, L., Powell, B., McIntosh, M., and Sanders, B., 2002, Dye tracing along major highways in Rutherford Co.: Planning for emergency spill response, *in* Proceedings, Tennessee Water Resources

Symposium, 12th: Nashville, Tennessee, American Water Resource Association, p. 2A-27–2A-33.

Pope, M.C., Read, J.F., Bambach, R., and Hofman, H.J., 1997, Late Middle to Late Ordovician seismites of Kentucky, southwest Ohio and Virginia: Sedimentary recorders of earthquakes in the Appalachian basin: Geological Society of America Bulletin, v. 109, p. 489–503, doi:10.1130/0016-7606(1997)109<0489:LMTLOS>2.3.CO;2.

Quigley, M.C., Bastin, S., and Bradley, B.A., 2013, Recurrent liquefaction in Christchurch, New Zealand, during the Canterbury earthquake sequence: Geology, v. 41, p. 419–422, doi:10.1130/G33944.1.

Rast, N., Ettensohn, F.R., and Rast, D.E., 1999, Taconic seismogenic deformation in the Appalachian Orogen and the North American Craton, *in* MacNiocaill, C., and Ryan, P.D., eds., Continental Tectonics: Geological Society, London, Special Publication 164, p. 127–137.

Reesman, A.L., and Stearns, R.G., 1985, Evaluation of the Beech Grove and a system of nearby lineaments in central Tennessee: Southeastern Geology, v. 26, p. 1–20.

Reesman, A.L., and Stearns, R.G., 1989, The Nashville dome, an isostatically induced erosional structure and the Cumberland Plateau Dome, an isostatically suppressed late Paleozoic extension of the Jessamine dome: Southeastern Geology, v. 30, p. 147–174.

Renne, P.R., Mundil, R., Balco, G., Min, K., and Ludwig, K.R., 2010, Joint determination of ^{40}K decay constants and ^{40}Ar*/^{40}K for the Fish Canyon sanidine standard, and improved accuracy for ^{40}Ar/^{39}Ar geochronology: Geochimica et Cosmochimica Acta, v. 74, p. 5349–5367, doi:10.1016/j.gca.2010.06.017.

Resor, P.G., 2008, Deformation associated with a continental normal fault system, western Grand Canyon, Arizona: Geological Society of America Bulletin, v. 120, p. 414–430, doi:10.1130/B26107.1.

Ryder, R.T., 1987, Oil and Gas Resources of the Cincinnati Arch, Ohio, Indiana, Kentucky, and Tennessee: U.S. Geological Survey Open-File Report 87-450Y, 30 p.

Sharp, I.R., Gawthorpe, R.L., Underhill, J.R., and Gupta, S., 2000, Fault-propagation folding in extensional settings: Examples of structural style and synrift sedimentary response from the Suez rift, Sinai, Egypt: Geological Society of America Bulletin, v. 112, p. 1877–1899, doi:10.1130/0016-7606(2000)112<1877:FPFIES>2.0.CO;2.

Sims, P., Saltus, R., and Anderson, E., 2008, Precambrian Basement Structure Map of the Continental United States: U.S. Geological Survey Scientific Investigations Map 3012, scale 1:8,000,000.

Stearns, R.G., and Reesman, A.L., 1986, Cambrian to Holocene structural and burial history of Nashville dome: American Association of Petroleum Geologists Bulletin, v. 70, p. 143–154.

Wayman, E., 2008, Lay of the land: Terrain's toll on the U.S. Civil War: Earth Magazine, v. 53, p. 52–59.

Wells, D.L., and Coppersmith, K.J., 1994, New empirical relationships among magnitude, rupture length, rupture width, rupture area, and surface displacement: Bulletin of the Seismological Society of America, v. 84, p. 974–1002.

Willsey, S.P., Umhoefer, P.J., and Hilley, G.E., 2002, Early evolution of an extensional monocline by a propagating normal fault: 3D analysis from combined field study and numerical modeling: Journal of Structural Geology, v. 24, p. 651–669, doi:10.1016/S0191-8141(01)00120-1.

Wilson, C.W., Jr., 1964, Geologic Map and Mineral Resources Summary of the Walterhill Quadrangle, Tennessee: Tennessee Division of Geology Geologic Quadrangle Map 315-NW, scale 1:24,000.

Wilson, C.W., Jr., 1965, Geologic Map and Mineral Resources Summary of the Murfreesboro Quadrangle, Tennessee: Tennessee Division of Geology Geologic Quadrangle Map, 315-SW, scale 1:24,000.

Wilson, C.W., Jr., 1991, The Geology of Nashville, Tennessee (2nd ed.): Tennessee Division of Geology Bulletin 53, 185 p.

Wilson, C.W., Jr., and Hughes, T.H., 1963, Geologic Map and Mineral Resources Summary of the Gladeville Quadrangle, Tennessee: Tennessee Division of Geology Geologic Quadrangle Map 314-SW, scale 1:24,000.

Wilson, C.W., and Stearns, R.G., 1963, Quantitative analysis of Ordovician and younger structural development of the Nashville dome, Tennessee: American Association of Petroleum Geologists Bulletin, v. 47, p. 823–832.

Wilson, C., Miller, R., and McCary, C., 1963, Geologic Map and Mineral Resources Summary of the Bethesda Quadrangle: Tennessee Division of Geology Geologic Quadrangle Map 63-SE, scale 1:24,000.

Withjack, M.O., and Schlische, R.W., 2006, Geometric and experimental models of extensional fault-bend folds, *in* Buiter, S.J.H., and Schreurs, G., eds., Analogue and Numerical Modelling of Crustal-Scale Processes: Geological Society, London, Special Publication 253, p. 285–305.

Withjack, M.O., Olson, J., and Peterson, E., 1990, Experimental models of extensional forced folds: American Association of Petroleum Geologists Bulletin, v. 74, p. 1038–1054.

Yin, A., 2004, Gneiss domes and gneiss dome systems, *in* Whitney, D.L., Teyssier, C., and Siddoway, C.S., eds., Gneiss Domes in Orogeny: Geological Society of America Special Paper 380, p. 1–14, doi:10.1130/0-8137-2380-9.1.

Manuscript Accepted by the Society 7 December 2014

Printed in the USA

Field Guides

A road guide to the Harpeth River and Stones River fault zones on the northwest flank of the Nashville dome, central Tennessee

Mark Abolins, Shaunna Young, Joe Camacho, Mark Trexler, Alex Ward, Matt Cooley and Albert Ogden

Field Guides 2015;39;1-20
doi: 10.1130/2015.0039(01)